

# Formulation of Deformable Liponiosomal Hybrid of Repaglinide: In vitro Characterization and Evaluation of the Anti-Diabetic Effect

Ali F Abdelwahab<sup>1</sup>, Alshimaa M Abdelmohymen<sup>2</sup>, Nada M Mostafa<sup>2</sup>, Galal Magdy<sup>3</sup>, Eman A Mazyed<sup>4</sup>

<sup>1</sup>Department of Pharmacology, Faculty of Medicine, Cairo University, Cairo, Egypt; <sup>2</sup>Department of Pharmacology, Faculty of Medicine, Beni-Suef University, Beni-Suef, Egypt; <sup>3</sup>Department of Pharmaceutical Analytical Chemistry, Faculty of Pharmacy, Kafrelsheikh University, Kafrelsheikh, Egypt; <sup>4</sup>Department of Pharmaceutical Technology, Faculty of Pharmacy, Kafrelsheikh University, Kafrelsheikh, Egypt

Correspondence: Eman A Mazyed, Tel +20 100 3484508, Email eman\_mazyad@pharm.kfs.edu.eg

**Purpose:** The current study sought to create novel deformable liponiosomal hybrids (LNHs) as a viable RPG delivery system. Repaglinide (RPG) is an effective anti-hyperglycemic drug. However, its limited solubility may limit its therapeutic applicability. LNHs are a potential liposome-niosome combination. Using phospholipids and non-ionic surfactants together improves their functionality in regulating drug release and increasing their permeability and stability.

**Materials and Methods:** The development of RPG-loaded LNHs was performed using the reverse ethanol injection method based on the 2<sup>3</sup> factorial design to explore the potential of various variables on the encapsulation efficiency (EE%) and % RPG released after 12 h (Q<sub>12h</sub>). Further in vitro characterization tests and in vivo study were also performed on the optimal RPG-loaded LNHs.

**Results:** After investigating how the examined independent factors could affect significantly both the EE % and Q<sub>12h</sub>, F7 was selected as the optimal liponiosomal formulation. F7 showed 87.07 ± 2.27 EE% and 94.32 ± 1.25 Q<sub>12h</sub>. F7 demonstrated higher permeability and stability than the corresponding liposomes and niosomes. Furthermore, F7 demonstrated greater hypoglycemic efficacy and bioavailability than pure RPG.

**Conclusion:** The combination of liponiosomes and niosomes in the form of LNHs has the potential to be an effective nano-drug delivery vehicle for RPG.

**Keywords:** repaglinide, liponiosomes, nano-drug delivery, diabetes

## Introduction

RPG is a carbamoyl benzoic acid derivative that belongs to the Meglitinide class, [Figure 1](#). It is extensively used as an anti-hyperglycemic drug for the management of non-insulin-dependent diabetic mellitus via induction of insulin secretion by binding to the pancreatic  $\beta$  cells.<sup>1</sup> However, its oral bioavailability is limited (56%) owing to its low solubility, poor absorption and significant hepatic first-pass effect, with a short half-life of 1 h. Furthermore, RPG is taken three to four times a day which reduces patient compliance.<sup>2</sup>

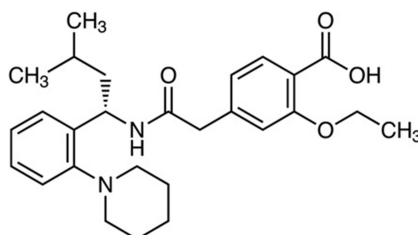


**Figure 1** The chemical structure of RPG.

**Abbreviation:** RPG, Repaglinide.

Nanoencapsulation has the potential to lower effectively the first-pass effect while boosting both the dissolution rate and drug stability.<sup>3</sup> There are different types of nano-vesicular drug delivery systems such as niosomes (surfactant-based nanovesicles) and liposomes (phospholipid-based nanovesicles) that have an amphiphilic nature. Hence, they act as efficient transporters for both hydrophilic and hydrophobic drugs.

The previous studies have fabricated the liposomal<sup>3</sup> and niosomal<sup>4</sup> carriers of RPG as controlled drug delivery systems. Each system has its own advantages and disadvantages. Liposomal vesicles are excellent nanocarriers due to their resemblance to cell membranes and low toxicity.<sup>5</sup> However, the niosomal carriers show superior physical and chemical stability profiles than the corresponding liposomes.<sup>6</sup> Accordingly, they require no specific storage conditions.<sup>7</sup> Liponiosomal hybrids (LNHs) are a promising combination of liposomes and niosomes. The amphiphilic liponiosomal vesicles have comprised of a phospholipid, non-ionic surfactant and cholesterol as a membrane stabilizer. Using both phospholipids and non-ionic surfactants has improved their functionality in regulating drug release and boosts their stability. Moreover, the characteristics of the liponiosomal vesicles are variable and controllable by altering the nanovesicle composition and concentration. Besides, the infrastructure of LNHs involved lipophilic, hydrophilic and amphiphilic components that permit the accommodation of drugs with wide solubility ranges.<sup>8</sup> There are few researches that have discussed the development of liponiosomes such as Sasani et al<sup>9</sup> who investigated the preparation of the liponiosomes as an efficient carrier of Doxorubicin HCl for the treatment of cancer. Mohammadi et al<sup>5</sup> also developed the liponiosomes of ginger extract for improving its anti-fungal activity. The current manuscript discussed the fabrication of ultra-deformable liponiosomes which are more advantageous than the conventional liponiosomes because they have the benefit of being more flexible to penetrate narrow pores of biological membranes without rupture of their vesicular membranes.<sup>10</sup> The higher flexibility of ultra-deformable LNHs is due to the addition of a destabilizing factor (the edge activator) to the vesicular membrane that enhances the membrane flexibility and drug permeability. This manuscript investigated the implication of deformable LNHs as a promising and innovative drug delivery approach for RPG to improve its efficacy as an anti-diabetic drug.

## Materials and Methods

### Materials

RPG was donated by the Egyptian International Pharmaceutical Industries Co., EPICO (Cairo, Egypt). Streptozotocin (STZ), Acetonitrile (ACN) (HPLC grade, > 99.9%), cholesterol (CHOL), Sorbitan monostearate (Span 60), sodium hydroxide, Polyoxyethylene lauryl ether (Brij 35), isopropyl alcohol, Polyoxyethylene (20) sorbitan monooleate (Tween 80), and phosphatidyl choline (PC) were purchased from Sigma Chemical Co. (St. Louis, MO, USA). Methanol, absolute ethyl alcohol, potassium dihydrogen phosphate, phosphoric acid, dipotassium monohydrogen phosphate, citric acid, and sodium citrate were purchased from El-Nasr Pharmaceutical Chemical Company (Cairo, Egypt). Analytical-grade solvents and chemicals were used throughout the study.

### Methods

#### HPLC Analysis of RPG-Loaded LNHs

##### Preparation of Standard Solution

Into a 100.0-mL volumetric flask, the stock solution of RPG (100.0 µg/mL) was prepared by dissolving 0.01 gm of the RPG standard pure powder in methanol. Serial dilution of the standard solution was performed using the mobile phase to prepare working solutions. Into a set of volumetric flasks (5.0 mL), volumes of 5.0, 10.0, 20.0, 50.0, 100.0, 200.0 µL were transferred from the prepared stock solution (100.0 µg/mL) and the flasks were completed to the mark with the mobile phase to prepare 6 different solutions with concentrations of 0.1, 0.2, 0.4, 1.0, 2.0, 4.0 µg/mL. All of which remained stable for at least two weeks when stored at a temperature of 4 °C.

#### Equipment and Software Utilized

A Dionex UltiMate 3000 HPLC device (Thermo Scientific™, Dionex™, Sunnyvale, CA, USA) was employed throughout this investigation. The system included a column thermostat (TCC-3000SD), an autosampler (WPS-3000TSL), a quaternary pump (LPG-3400SD), and a fluorescence detector (FLD-3100 Dual-PMT). For data collection and

processing, Chromeleon 7 software was used in conjunction with a Hypersil BDS C18 column (250 mm x 4.6 mm i.d., 5  $\mu$ m particle size). Additional instruments required for this study included a vortex mixer (model IVM-300p, Gemmy Industrial Corp, Taiwan), a cooling centrifuge (model 2-16P, Germany), a pH meter (Jenway 3510, UK), as well as a membrane filter featuring a 0.45  $\mu$ m pore size (Phenomenex, USA).

### Chromatographic Conditions

RPG detection was achieved using a reversed-phase C18 column (Hypersil BDS; particle size: 5  $\mu$ m; dimensions: 250  $\times$  4.6 mm i.d.) and a mobile phase consisting of methanol, acetonitrile, and potassium dihydrogen phosphate buffer (0.01 M, pH 2.5, adjusted using phosphoric acid) at a volumetric ratio of 18:51:31 (%v/v). Isocratic elution proceeded with a flow rate of 1.5 mL/min and a 20.0  $\mu$ L sample injection volume. The fluorescence detector was set at 245/350 nm ( $\lambda$  excitation/ $\lambda$  emission), and column conditioning for 20 min prior to the assay was necessary. Figure 2 shows HPLC chromatogram of RPG under the optimum chromatographic conditions.

### Construction of Calibration Graph (Aqueous Samples)

Varying known quantities of the RPG standard solution (100.0  $\mu$ g/mL) were transferred into volumetric flasks (5.0 mL) and subsequently diluted with the mobile phase, forming solutions in a concentration range of 0.1–4.0  $\mu$ g/mL. Under optimal chromatographic conditions, triplicate injections were performed for each solution, consisting of 20.0  $\mu$ L volumes in total. The calibration curve was derived by plotting the drug concentrations ( $\mu$ g/mL) against their respective peak area.

### Preparation and Optimization of RPG-Loaded LNHs

The reverse ethanol injection method was employed for RPG-loaded liponiosomal hybrid formulation. PC and Span 60 mixture were used to develop a spherical lipid bilayer of the RPG-loaded LNHs. CHO was employed as membrane stabilizer to improve the rigidity of the vesicular membrane. Briefly, accurate weights of RPG, PC, CHO, and Span 60 were dissolved in 2 mL ethanol, as shown in Table 1. An appropriate amount of preheated distilled water (60  $^{\circ}$ C), with/without the addition of EA (Tween 80), was dropped continuously into the alcoholic lipid solution while being shaken using Jenway magnetic stirrer (Jenway 1000, Jenway, UK). The stirring process was continued at room temperature for 1 h, in order to confirm the total elimination of ethanol. The LNH dispersion was sonicated at room temperature using a bath sonicator (Elmasonic E 30 H, Elma, Singen, Germany) for 10 minutes. The LNHs were kept overnight in a refrigerator for complete maturation.

The 2<sup>3</sup> factorial design is two-level (low and high), three-variable design. The study involved eight runs and each experiment was performed in triplicate (n = 3), then the results were described as mean  $\pm$  standard deviation (SD) by averaging the outcomes. The analysis of variance (ANOVA) was used to explore the statistical significance of the results.

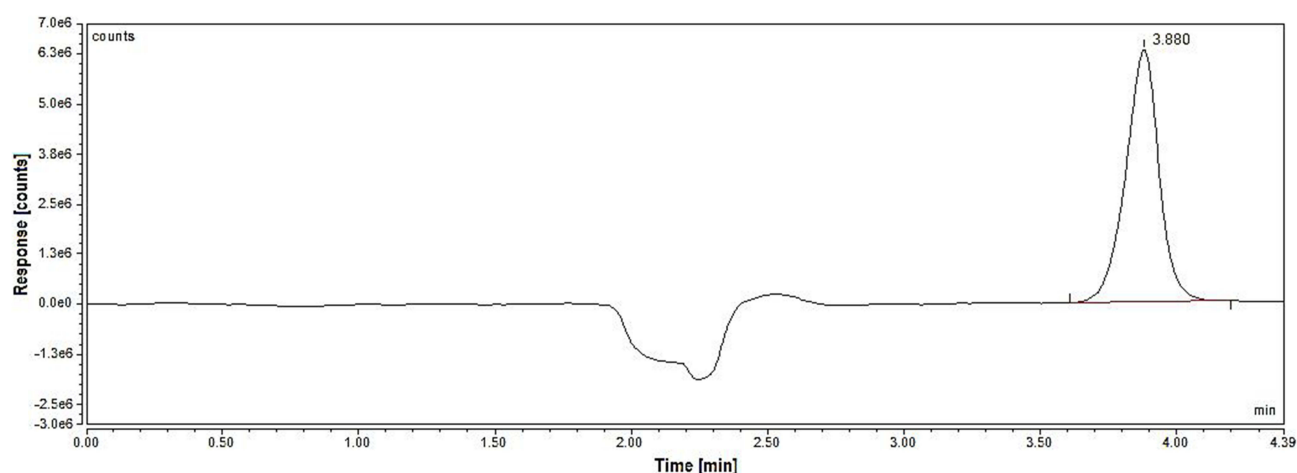


**Figure 2** Typical chromatogram of RPG (1.0  $\mu$ g/mL) under the optimum chromatographic conditions.

**Abbreviation:** RPG, Repaglinide.

**Table 1** The Factorial Design for RPG-Loaded LNHs Involving the Experimental Runs and Independent Variables

Formula	Independent Variables		
	X1	X2	X3
F1	−I	−I	−I
F2	−I	I	−I
F3	−I	−I	I
F4	−I	I	I
F5	I	−I	−I
F6	I	I	−I
F7	I	−I	I
F8	I	I	I
Independent variables		Low (−I)	High (+I)
X1: Weight of Span (mg)		200	300
X2: Weight of PC (mg)		100	200
X3: Weight of EA (mg)		0	100

**Note:** All formulations involved 50 mg CHO and 10 mg RPG.

**Abbreviations:** PC, phosphatidylcholine; EA, edge activator.

Optimizing the RPG-loaded LNHs with the  $2^3$  factorial design by the Design-Expert software (Version 7.0.0, Stat-Ease, Inc., Minneapolis, MN, USA) has investigated the influence of the specified independent variables on the studied responses (encapsulation efficiency (EE%) and the % RPG released after 12 h ( $Q_{12h}$ )).

## In Vitro Evaluation of RPG-Loaded LNHs

### Estimation of EE% of LNHs of RPG

The EE% of LNHs of RPG was evaluated by separating the un-entrapped RPG using the indirect approach of ultracentrifugation [37] at 4 °C (cooling centrifuge, Biofuge, Primo Heraeus, Germany) for 1h at 20,000 rpm. The supernatant layer was then separated carefully and filtered (0.45 µm Nylon syringe filter, Gelman Sciences Inc., MI, USA). The concentration of free RPG in the supernatant was estimated using HPLC with fluorescence detection at 245/350 nm ( $\lambda$  excitation/ $\lambda$  emission) in about 3.8 min. The EE% was estimated via the following equation:

$$EE(\%) = (R_t - R_s) \times 100 / R_t \quad (1)$$

where  $R_t$  = total amount of RPG,  $R_s$  = amount of RPG in the supernatant.

The total content of RPG within the LNHs was also determined by disrupting the RPG-loaded LNHs (0.5 mL) using 50 mL isopropyl alcohol.<sup>11,12</sup> The alcoholic dispersion was stirred using a magnetic stirrer (Jenway 1000, Jenway, UK) for 24 h. The dispersion was filtered (0.45 µm Nylon syringe filter, Gelman Sciences Inc., MI, USA) and HPLC was used to determine the concentration of free RPG in the supernatant with fluorescence detection at 245/350 nm ( $\lambda$  excitation/ $\lambda$  emission).

## In vitro Release of RPG-Loaded LNHs

The membrane diffusion technique<sup>13</sup> was selected to study the in vitro release of RPG from the LNHs, Figure 3. The approach involves attaching a prehydrated cellulose dialysis membrane (MWCO; 12,000 to 14,000 Dalton, Spectrum Laboratories Inc., U.S.A.)<sup>14</sup> to the base of a glass cylinder. The glass cylinder was then fixed to the shaft of USP dissolution apparatus II (Erweka DT-720, Langen, Germany).<sup>7</sup> The receptor compartment was packed by the dissolution medium (phosphate buffer (300 mL, pH = 7.4))<sup>15</sup> containing 0.5% Brij 35 for the fulfillment of sink conditions.<sup>16</sup> The receptor



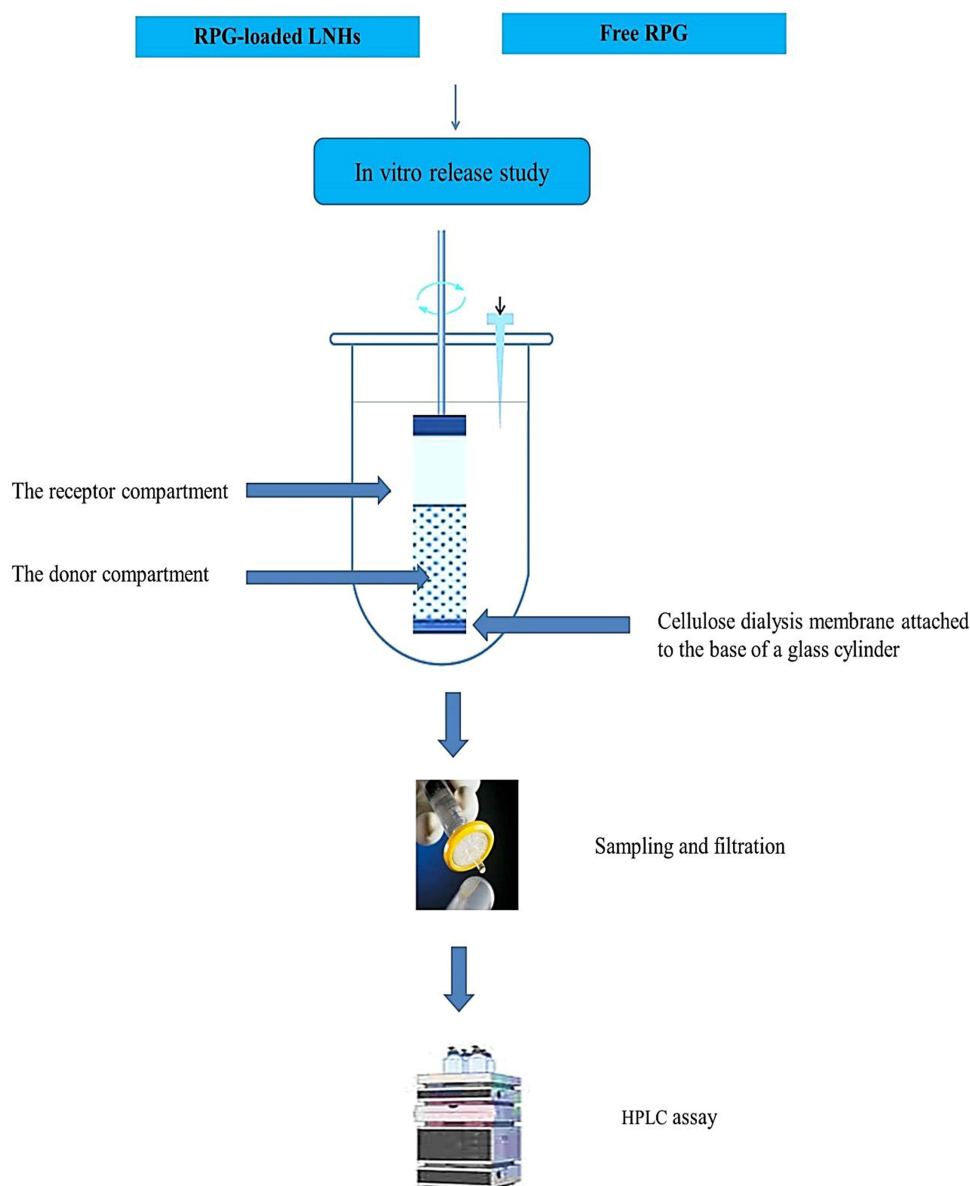


**Figure 3** Schematic illustration of the in vitro release study of RPG-loaded LNHs and RPG dispersion across the cellulose membrane.

**Abbreviations:** RPG, Repaglinide; LNHs, Liponiosomal hybrids of Repaglinide.

chamber was retained at  $37 \pm 1$  °C with constant agitation at 50 rpm. A sample of the RPG-loaded LNHs (1 mL) was added to the donor chamber over the cellulosic dialysis membrane. At the predetermined intervals, a 2 mL sample was withdrawn and consistently replaced with an equal volume of freshly prepared phosphate buffer.<sup>17</sup> The RPG samples were filtered (0.45 µm Nylon syringe filter, Gelman Sciences Inc., MI, USA) and HPLC was used to calculate the concentration of free RPG in the supernatant with fluorescence detection at 245/350 nm ( $\lambda$  excitation/ $\lambda$  emission). The study was conducted in triplicate.

## Optimization of LNHs of RPG

The assessment of the optimal LNHs of RPG was performed by calculating the total desirability based on the uppermost values of both EE% and  $Q_{12h}$ .<sup>18</sup> The highest desirability value of the optimal LNHs explored the nearness of the observed responses to their ideal values. The optimized liponiosomal formula of RPG was subsequently put through more characterization tests.

## Characterization of the Optimized LNHs of RPG

### Vesicle Size and Zeta Potential Estimation

About 100 mL of the deionized water was used to properly dilute a 1 mL aliquot of the optimal liponiosomal formula of RPG. The samples were measured using a NICOMP 380 ZLS zeta potential/particle sizer at 25°C (PSS-Nicom, Santa Barbara, CA, USA) at a 90° dispersing angle. The measurements were performed in triple.<sup>19</sup>

### Morphological Characterization by Scanning Electron Microscopy (SEM)

The SEM was used to describe the morphological characteristics of the optimized RPG-loaded LNHs (JSM 6100 JEOL, Scanning electron microscope, Tokyo, Japan). A sample of 1 mL of LNHs of RPG was properly diluted by 100 mL of deionized water. On the SEM specimen stub, a drop of the dilute LNHs of RPG was gently applied. After that, the liponiosomal sample was air-dried before SEM scanning.<sup>20</sup>

### Measurement of Elasticity of Liponiosomal Vesicles

In comparison to the corresponding NVs and LVs, the elasticity of the optimal RPG-loaded LNHs was assessed using the extrusion technique for 5 min by calculating the deformability index (DI)<sup>21</sup> as follows:

$$DI = J(r_v/r_p)^2 \quad (2)$$

Where J is the volume of the extruded liponiosomal of RPG,  $r_v$  represents the size of the extruded liponiosomal vesicles, and the membrane filters' pore size is represented by  $r_p$ .

### Ex vivo Intestinal Permeability Study

The intestinal permeability testing was done to explore how the LNHs affected the permeability of RPG, [Figure 4](#). Ethical standards were followed upon conducting the intestinal permeability test.<sup>22–24</sup> The test protocol was also authorized by the ethical committee of the Faculty of Medicine, Beni-Suef University, Egypt (approval number: 021–206). Under anaesthesia, the rats (male Wistar rats;  $n = 6$ , 200–220 g) were slaughtered. The small intestines were meticulously excised and properly cleansed with 0.9% sodium chloride solution to get rid of any extra mucosal material.<sup>25,26</sup> The excised small intestines were divided into tiny sacs. The investigated samples (1 mL) were placed into the intestinal sacs. Surgical threads were used to suture the sac ends. The intestinal sacs were securely fastened to the shafts of the USP dissolution equipment.<sup>25,27</sup> The receptor medium for the ex vivo intestinal permeability testing of RPG-loaded LNHs was 200 mL of 0.5% Brij-containing phosphate buffer with a pH of 7.4.<sup>15</sup> The receptor chamber was retained at  $37 \pm 1$  °C with continuous agitation at 50 rpm. At the predetermined intervals, a 2 mL sample was taken out and replaced on a regular basis by an equal volume of freshly prepared phosphate buffer. The samples were then filtered (0.45 µm Nylon syringe filter, Gelman Sciences Inc., MI, USA) and assayed by HPLC for the amount of permeated RPG with fluorescence detection at 245/350 nm ( $\lambda$  excitation/ $\lambda$  emission). The intestinal permeation parameters<sup>7,12</sup> of LNHs of RPG were also compared with the RPG suspension, as well as the niosomal and liposomal preparations of RPG.

### Fourier Transform Infrared Spectroscopy (FTIR)

A mixture of the studied component with potassium bromide was compressed using a hydraulic press (Kimaya Engineers, Maharashtra, India). The IR spectra of RPG, the selected excipients, the physical mixture, and the optimized formula were detected using the IR spectrometer (FT-IR Shimadzu 8300 Japan) within 4000–400  $\text{cm}^{-1}$  scanning range.<sup>28</sup>

### The Stability Testing

The optimal liponiosomal formula and the corresponding NVs and LVs were stored at 4 °C for a period of three months in tightly sealed bottles. The impact of the synergism between the niosomal and liposomal ingredients on the stability of LNHs of RPG was investigated.

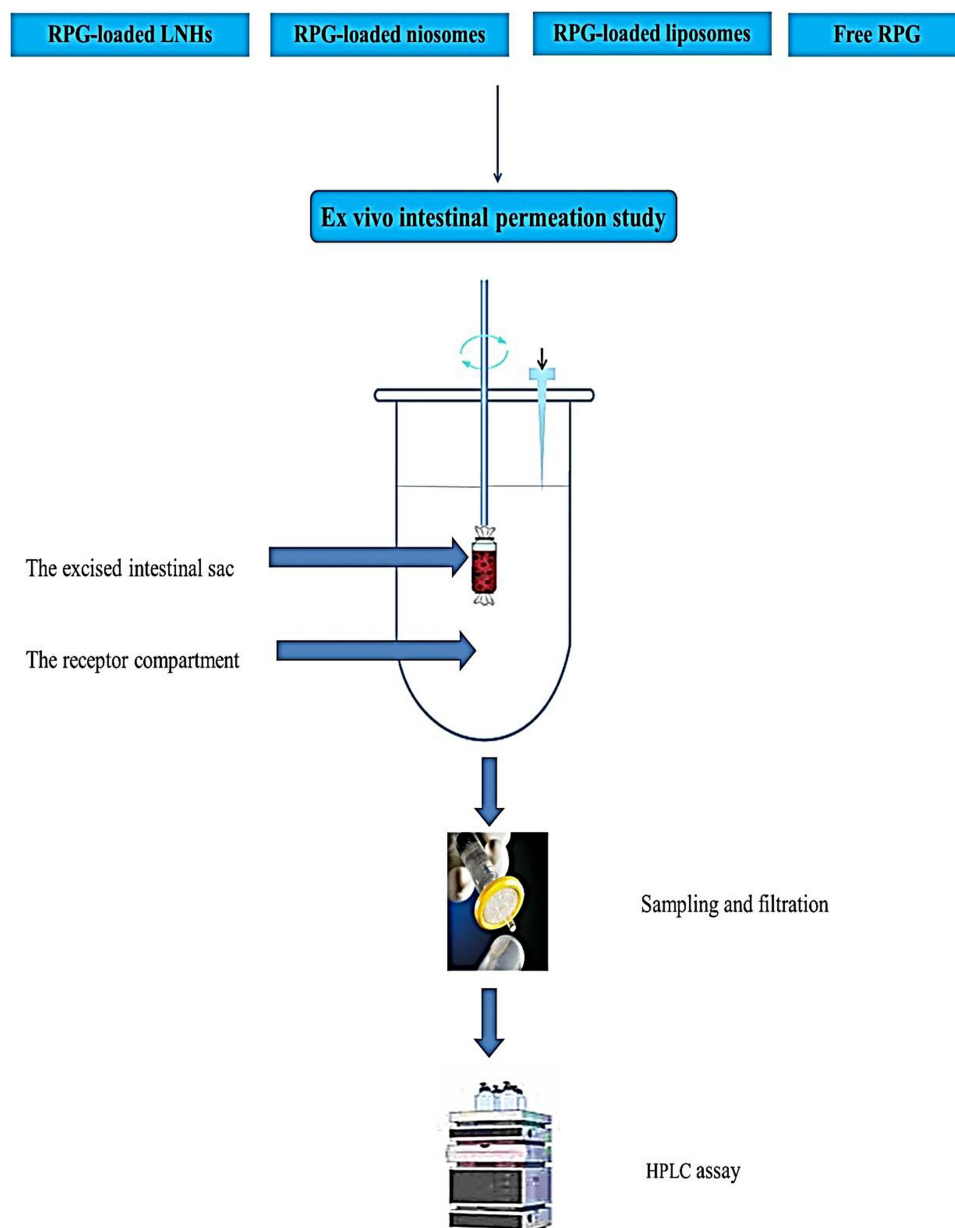


**Figure 4** Schematic illustration of the intestinal permeation study of RPG-loaded LNHs, RPG-loaded niosomes, RPG-loaded liposomes and RPG dispersion.  
**Abbreviations:** RPG, Repaglinide; LNHs, Liponiosomal hybrids of Repaglinide.

## In vivo Study

### Animals

A total of thirty-six adult male Westar albino rats, weighing 100–120 g, were kept in a pathogen-free environment with a constant temperature of 25°C, subjected to 12-hour dark/light cycles, and granted unrestricted access to water. A high-fat diet (HFD) was given to the rats in accordance with the experimental design. The handling of animals and the applied procedures followed the ethical guidelines of the National Institutes of Health (NIH),<sup>29</sup> European Union Directive 2010/63/EU, and the ARRIVE guidelines<sup>23,24</sup> and gained approval from the ethical committee of Beni-Suef University (approval number: 021–206). The rats were acclimatized for a week before random allocation into different groups.

## High-Fat Diet (HFD)

The HFD was prepared by mixing 1000 g of the powdered normal pellet diet (NPD), 125 g of casein, 531 g of butter, 7 g of vitamin mix, 3 g of DL-methionine, and 42 g of mineral mix ([Tables S1](#) and [S2](#)).<sup>30</sup>

## Experimental Design

The study was conducted as two sets of experiments to study the effect of encapsulating RPG within LNHs on both the therapeutic efficiency and the pharmacokinetic profile.

## Assessment of Therapeutic Efficiency of RPG and RPG-Loaded LNHs

Twenty-four rats were randomly categorized into four groups, each consisted of six rats, [Figure 5](#). Group 1: Normal control group (fed by a regular diet and received only citrate buffer); Group 2: DM control group (fed by a HFD and received STZ alone); Group (3) pure RPG-treated group (diabetic rats received pure RPG dissolved in distilled water in a dose of (2mg/kg) orally through a gastric tube). Group (4) LNHs of RPG-treated group (diabetic rats received LNHs of RPG in a dose equivalent to 2mg/kg RPG through gastric tube). Treatments continued for 14 days.<sup>31</sup>

## STZ-Induced Type 2 Diabetes in Rats

Type 2 DM was induced in the rats using STZ by feeding them a HFD for three weeks to trigger insulin resistance. On Day 21, STZ was freshly dissolved in sodium citrate buffer (0.1 M, pH = 4.5) and injected, at a dose of 45 mg/kg, intraperitoneally.<sup>32</sup> Following the injection, animals were granted free access to 20% glucose in their drinking water for two days to counteract hypoglycemia.<sup>33</sup> After this period, rats with blood glucose levels ranging from 200 mg/dL to 480 mg/dL, as measured by a glucometer, were considered diabetic (Vanamedica Co, Cairo, Egypt).<sup>34,35</sup>

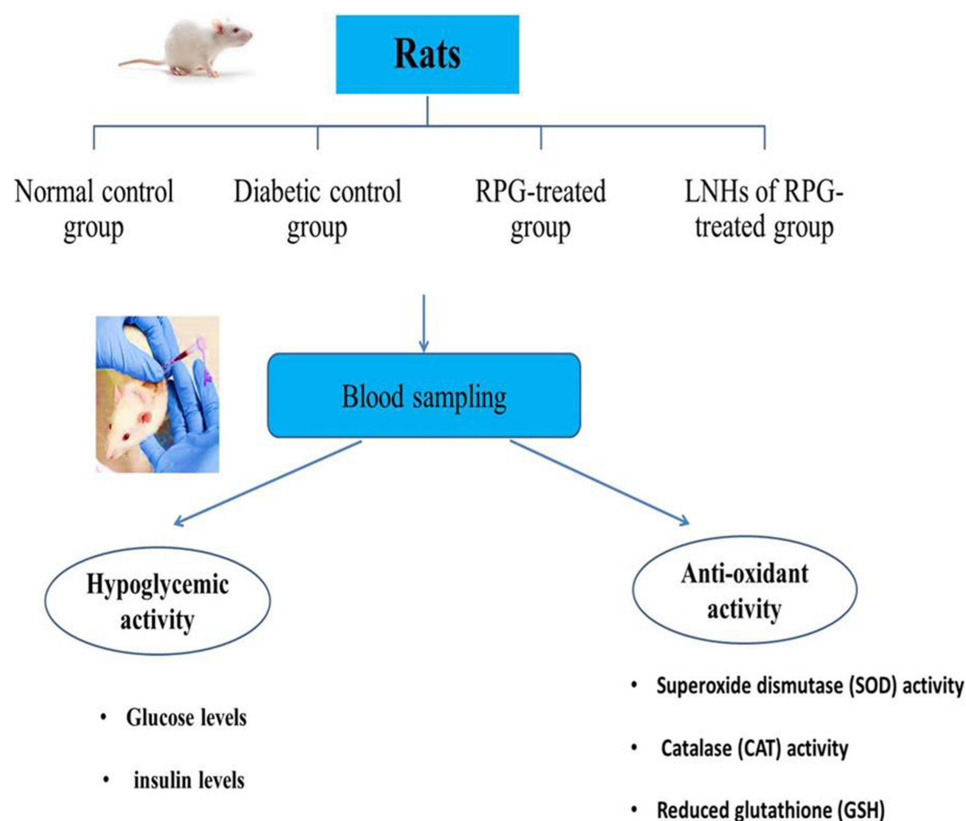


**Figure 5** Schematic illustration of the evaluation of the hypoglycemic activity and anti-oxidant activity in the serum of normal rats, diabetic control rats and those treated with pure RPG and RPG-loaded LNHs.

**Abbreviations:** RPG, Repaglinide; LNHs, Liponiosomal hybrids of Repaglinide.

## Blood Sampling

Upon completion of the test, blood specimens were obtained utilizing the retro-orbital puncture method under mild ether anesthesia at designated intervals. These intervals included 0, 1, 2, 4, 8, and 12h time points. The purpose of this collection process was to evaluate both the glucose percentage (mg/dL) and insulin concentration (ng/mL). Samples were incubated at 37°C until the blood clotting, centrifuged for 20 min at 4000 rpm, and then serum was separated to assess the glucose percent and insulin level. 24h following the last RPG dose, up to 4 mL sample volume was obtained and allowed to cool for 15 minutes in order to facilitate appropriate serum separation via clotting. Next, samples were centrifuged at 4000 rpm for a duration of 20 min to separate serum. This resulting serum was placed into sterile containers with subsequent biochemical evaluations conducted for superoxide dismutase (SOD) activity, catalase (CAT) activity, and reduced glutathione (GSH) concentrations. Finally, scarification of the tested rats was performed via decapitation utilizing a rodent guillotine.<sup>36</sup>

## Methods for Biochemical Study

Serum insulin concentrations were evaluated with the use of the Rat INS (Insulin) ELISA Kit (Catalog No: E-EL-R246696T). Additionally, anti-oxidative stress parameters including; CAT activity, SOD activity, and GSH concentration were measured using the colorimetric method.

## Study of Pharmacokinetic Profile of RPG and LNHs of RPG

Figure 6 summarizes the study of pharmacokinetic profile of RPG and LNHs of RPG. Twelve test subjects were arbitrarily assigned into two groups consisting of six rats each. Both groups received a standard diet for a five-day period. On the fifth day, single-dose oral pharmacokinetic examinations were conducted under fasted conditions; rats had been fasted for 23 hours prior to dosing and continued for an additional 10 hours post-dosing in line with Jinno et al, 2006.<sup>37</sup> Dosing procedures were as follows: Group (a): rats received pure RPG in a dose of 2mg/kg through gastric tube. Group (b): rats received LNHs of RPG in a dose equivalent to 2mg/kg RPG through gastric tube.<sup>31</sup> Blood specimens were procured from the retro-orbital plexus at 0 (pre-dose), 1, 2, 4, 8, and 12 h post-dose. These samples were collected in EDTA tubes to inhibit clotting and then centrifuged at 7000 rpm for a duration of 20 minutes at a temperature of 4°C. Plasma was subsequently separated and preserved at -20°C.

## Procedure for Plasma Samples

Separate aliquots of rat plasma samples (250.0 µL) were placed individually into distinct centrifugation tubes (2.0 mL). A 50.0 µL volume from the RPG stock solution was incorporated to achieve final concentrations ranging between 0.1 and 0.8 µg/mL. The spiked samples were vortexed for two minutes, followed by protein precipitation initiation by filling the centrifugation tubes to 1 mL with methanol. All tubes were subjected to centrifugation for a duration of 10 minutes at 10,000 rpm. The resulting supernatants were filtered utilizing 0.45 µm syringe filters, leading to drug concentration measurements executed as previously detailed and the corresponding regression equations were derived. HPLC chromatogram of RPG in plasma samples is illustrated in Figure 7.

The same procedure was employed in the preparations of real rat plasma samples, transferring 250 µL of each specimen into separate centrifugation tubes (2.0 mL). Post two-minute vortexing, protein precipitation was induced, reaching a volume of 1 mL by incorporating methanol into the centrifugation tubes. Centrifugal motion ensued for a period of 10 min at a velocity of 10,000 rpm. Supernatant filtration was performed through the use of 0.45 µm syringe filters and 20.0 µL of the finally prepared sample solution was injected to the HPLC system.

## Statistical Analysis

Statistical evaluations of the data were conducted utilizing ANOVA through the application of SPSS-11 software (SPSS, Inc., Chicago, IL, USA). The information gathered from the factorial design involving RPG-loaded LNHs was subjected to analysis via ANOVA, employing the Design-Expert software (Version 7.0.0, Stat-Ease, Inc., Minneapolis, MN, USA).

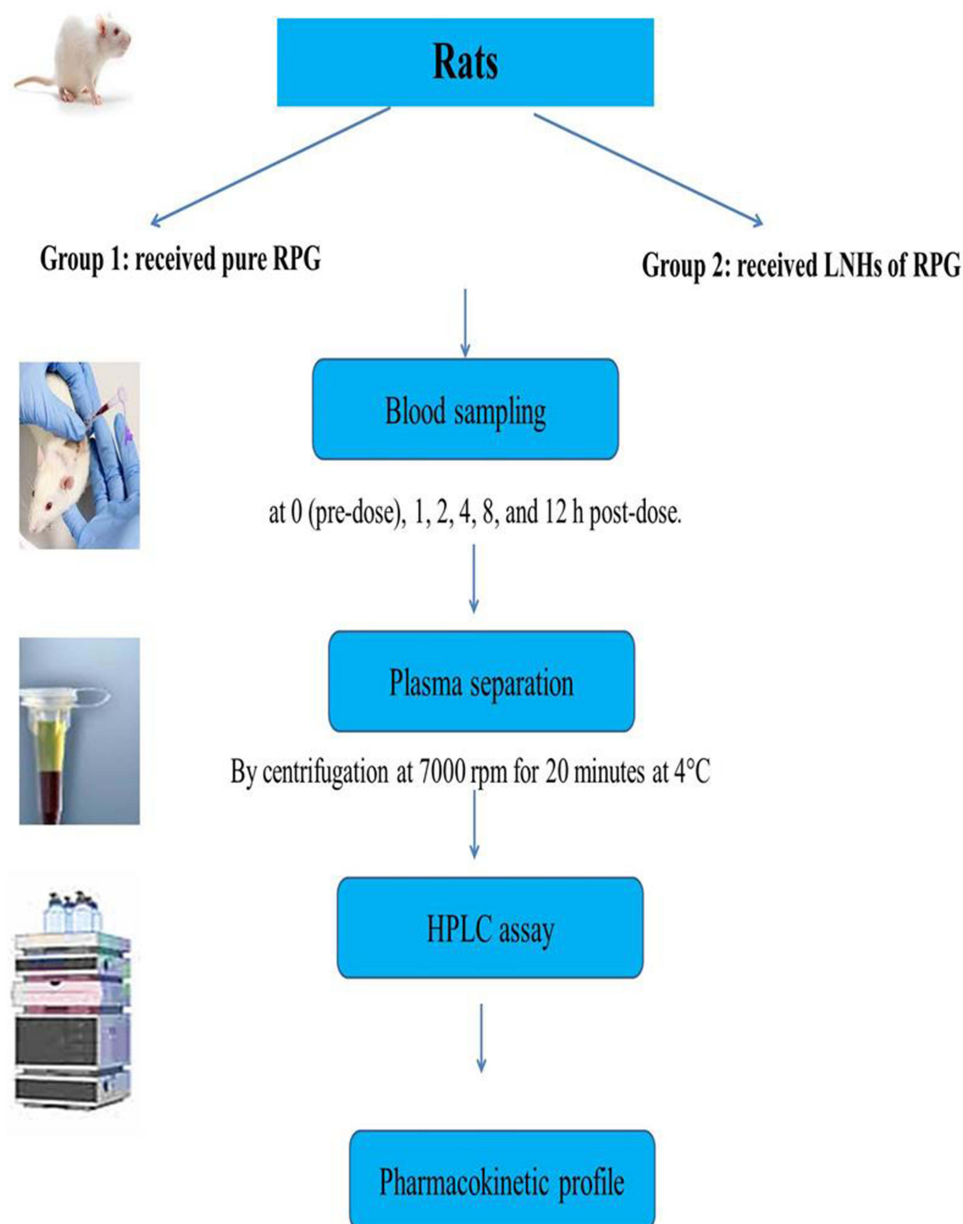


**Figure 6** Schematic illustration of the study of the pharmacokinetic profile of pure RPG and RPG-loaded LNHS.

**Abbreviation:** RPG, Repaglinide; LNHS, Liponiosomal hybrids of Repaglinide.

## Results and Discussion

### Optimization Study of RPG-Loaded LNHS Using the $2^3$ Factorial Design

Factorial designs are an effective tool for optimizing the pharmaceutical formulations by simultaneously testing various factors and their interactions. They can result in saving time, money, and resources by lowering the number of trials required to produce reliable findings. The  $2^3$  factorial design was applied in order to explore the most suitable values for the studied variables required to produce the LNHS of proper quality by studying how could the selected independent variables alter the properties of RPG-loaded LNHS; EE% (coded as Y1) and  $Q_{12h}$  (coded as Y2), Table 2.

The high values of adequate precision, for both responses suggest the capability of the current model in exploring the design space, Table 3. The outcomes exhibited high  $R^2$  of 0.9866 and 0.9714 which demonstrated the statistical validity of the derived equations and their good fit to the measured data. Additionally, the small difference between the predicted ( $Pred. R^2$ ) and adjusted  $R^2$  (Adj.  $R^2$ ) values investigated a respectable level of harmony among them.



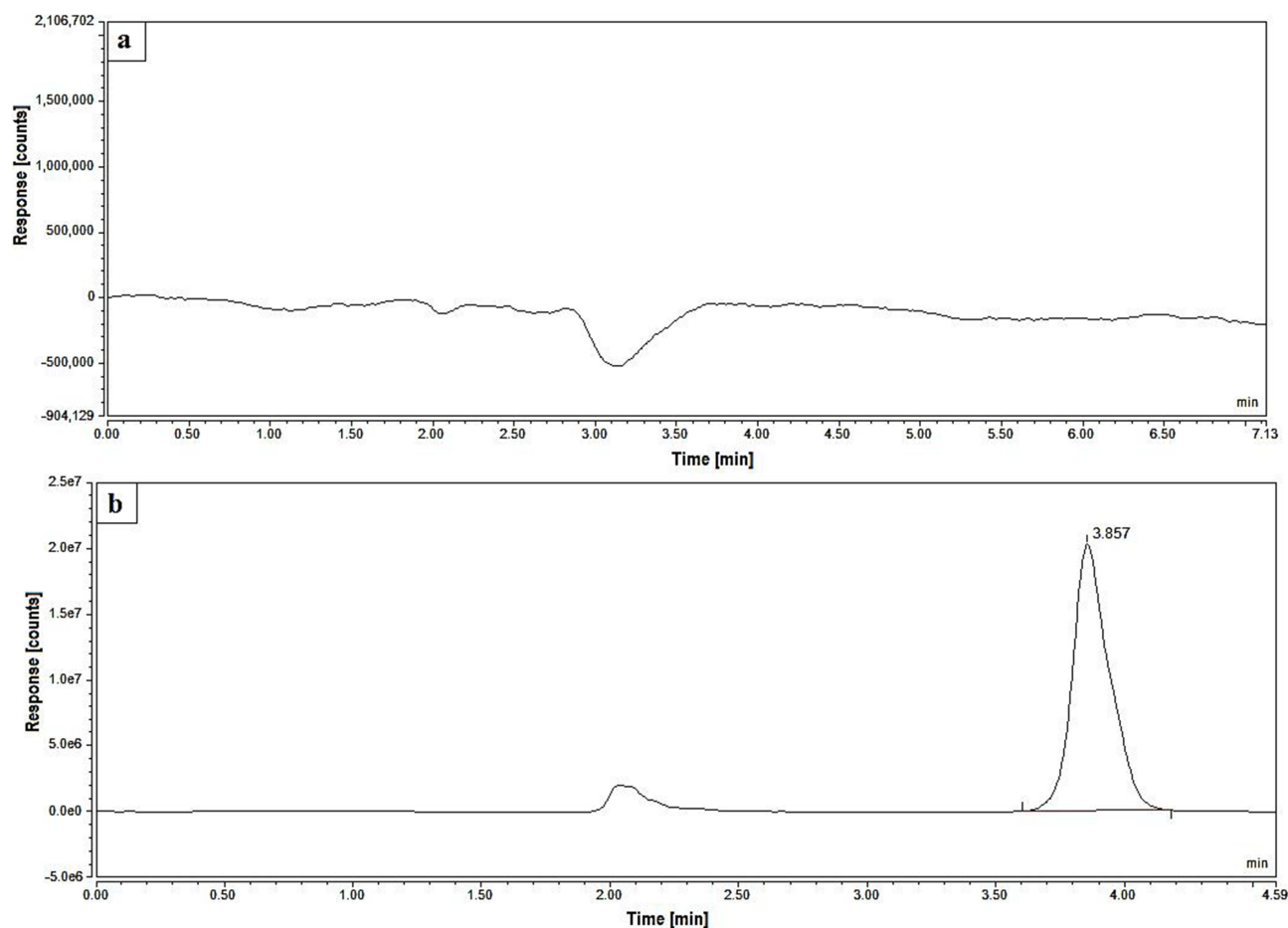


**Figure 7** Typical chromatograms of: (a) Blank plasma, (b) RPG (0.4 µg/mL) in rat plasma under the optimum chromatographic conditions.

**Abbreviation:** RPG, Repaglinide.

Additionally, Figures 8 and 9 investigate a linear correlation between the predicted responses (EE% and  $Q_{12h}$ , respectively) of RPG-loaded LNHs versus their corresponding observed values and the absence of the lurking variables due to uniform scattering of their residuals.

**Table 2** The Observed Values of % Encapsulation Efficiency and % RPG Released After 12h of the Studied LNHs

Formula	Responses	
	Y1*	Y2*
F1	69.58 ± 1.43	94.37 ± 2.46
F2	81.08 ± 1.75	83.37 ± 1.88
F3	78.40 ± 1.24	98.68 ± 1.55
F4	85.64 ± 1.36	91.20 ± 1.28
F5	82.72 ± 1.33	90.58 ± 1.62
F6	92.37 ± 1.19	78.96 ± 1.09
F7#	87.07 ± 2.27	94.32 ± 1.25
F8	97.37 ± 1.47	87.23 ± 1.36

**Notes:** \* the measurements (n = 3) are displayed as mean ± SD; Y1: EE (%), Y2:  $Q_{12h}$  (%), #The Optimized RPG-loaded LNHs.

**Table 3** The Coefficients of Determination and Adequate Precision of the 2<sup>3</sup> Factorial Design of the LNHNs of RPG

Responses	R <sup>2</sup>	Adj. R <sup>2</sup>	Pred. R <sup>2</sup>	Adeq. Precision
Y1 (EE%)	0.9866	0.9765	0.9462	28.69
Y2 (Q <sub>12h</sub> )	0.9714	0.9500	0.8857	19.18

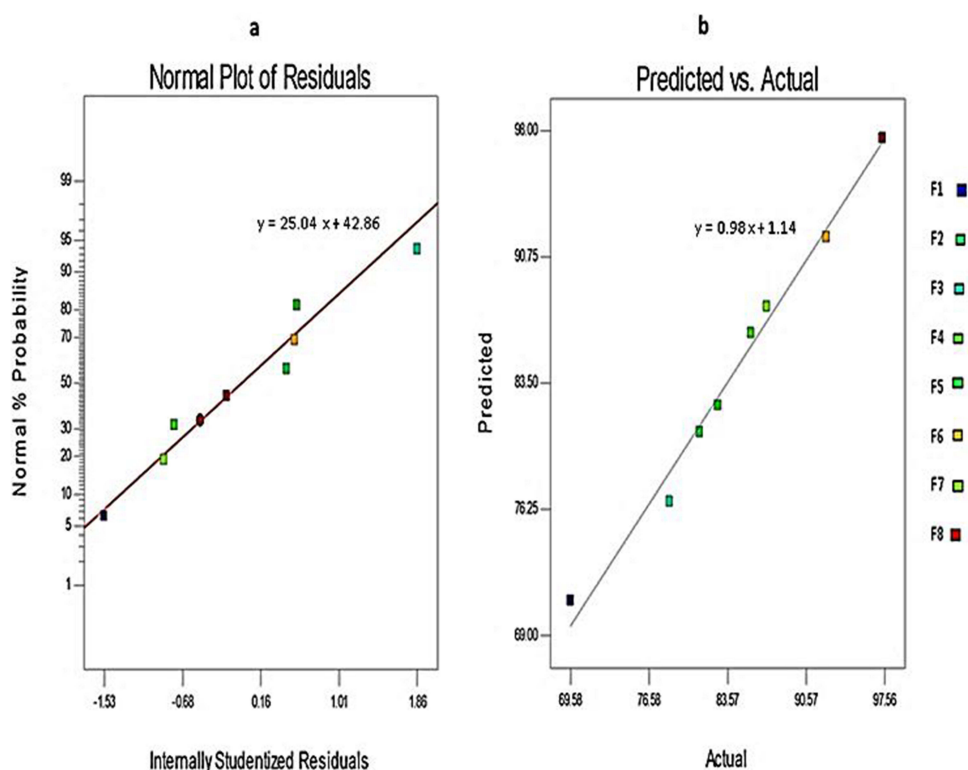
**Abbreviations:** EE%, percentage of encapsulation efficiency of RPG within LNHNs; Q<sub>12h</sub>, % RPG released after 12h; R<sup>2</sup>, the determination coefficient; Pred., predicted; Adj., adjusted; Adeq. Precision, Adequate precision.

## Data Analysis of EE% of RPG-Loaded LNHNs

The EE% of LNHNs of RPG ranged from  $69.58 \pm 1.43$  to  $97.37 \pm 1.47\%$ , Table 2 with a total content of 95.22–101.47%. The EE% of RPG-loaded LNHNs was analyzed at different levels of the studied variables. The influence of the designated variables on the values of EE% of LNHNs of RPG is investigated in the 3D plots (Figure 10). The 3D surface plots are three-dimensional charts that could effectively describe the relationship between the studied response and the independent variables in order to determine the best conditions for preparing the optimized pharmaceutical formulation. The 3D surface plot involves the selected variables on the x- and y-axes and a smooth surface representing the response values on the z-axis.

The 3D plot and ANOVA statistical data suggests that the amount of Span and the amount of PC had a substantial favorable impact ( $p < 0.001$ ) on the %EE of RPG, Table 4. This could be explained by increasing the rigidity of the liponiosomal bilayer and reducing RPG leakage from LNHNs.<sup>7</sup>

In terms of the amount of EA, it is obvious that the addition of EA improved the EE% of RPG ( $p < 0.01$ ). These findings could be attributable to the EA's intrinsic capabilities as a solubilizer, as well as interactions between the EA and the liponiosomal lipid bilayer<sup>38</sup> that minimize the leaking of RPG from the LNHNs.

**Figure 8** The normal probability plot (a) and the relation between the predicted and observed EE% (b) of RPG-loaded LNHNs.

**Abbreviations:** RPG, Repaglinide; EE, encapsulation efficiency of RPG-loaded LNHNs.

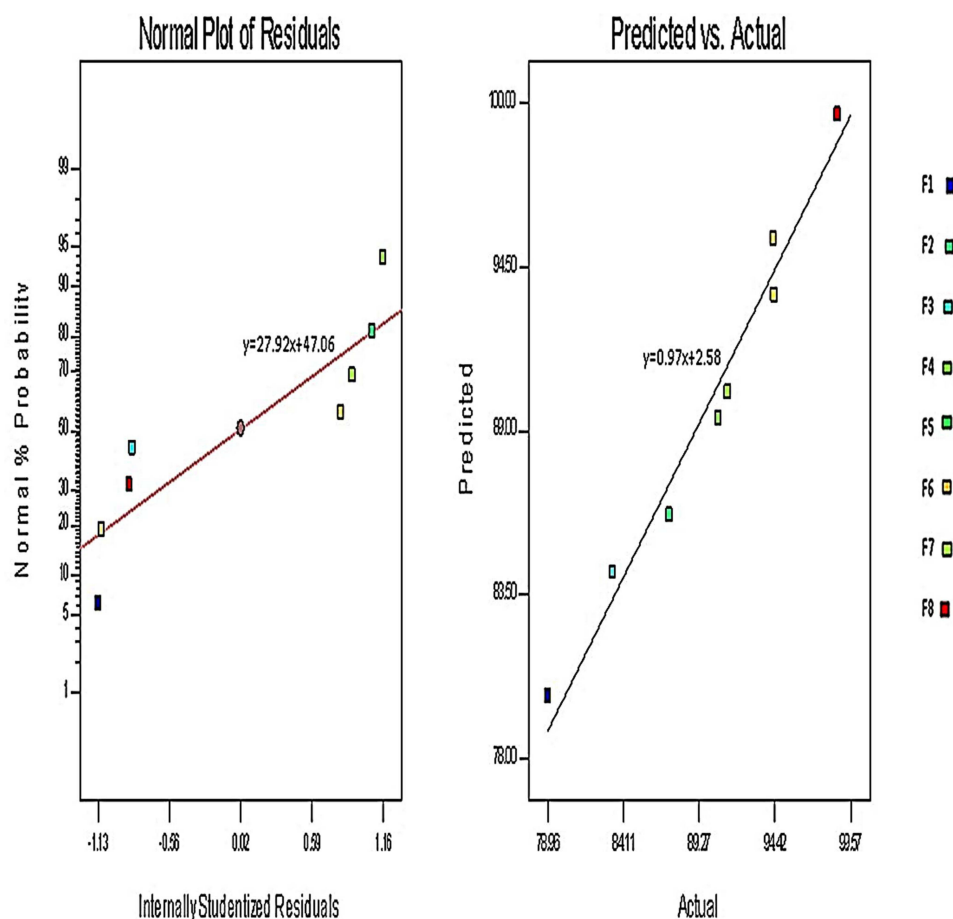


**Figure 9** The normal probability plot (a) and the relation between the predicted and observed  $Q_{12h}$  (b) of RPG-loaded LNHS.

**Abbreviations:** RPG, Repaglinide;  $Q_{12h}$ , % RPG released after 12h.

## Data Analysis of $Q_{12h}$ of RPG-Loaded LNHS

According to Figure 11, the formulated LNHS of RPG had  $Q_{12h}$  values ranging from  $78.96 \pm 1.09$  to  $98.68 \pm 1.55\%$ . The RPG in vitro release was more sustained than the free RPG that showed  $92.09 \pm 1.59\%$  drug released after 4h. These outcomes demonstrated the reservoir efficacy of the fabricated LNHS for controlling RPG release as well as the achievement of sink conditions.<sup>12</sup> These findings corroborated those of Eaknai et al<sup>10</sup> who reported that LNHS of Fenugreek extract exhibited a slower release profile than the Fenugreek extract.

The 3D plot (Figure 12) and ANOVA outcomes (Table 4) investigate the influence of the chosen variables on  $Q_{12h}$ . The quantity of PC exhibited a notable negative impact ( $p < 0.05$ ) on the percentage of RPG released. The Span 60 amount also showed a substantial adverse influence on  $Q_{12h}$  of LNHS ( $p < 0.001$ ). This could be related to increasing the liponiosomal bilayer stiffness, which limits the RPG efflux from LNHS.<sup>39</sup>

Regarding the quantity of EA, it is obvious that the LNHS have a significantly higher  $Q_{12h}$  than the analogous LNHS with  $p < 0.01$ . This might be attributed to improving the deformability of LNHS after adding EAs.<sup>28</sup>

## The Optimization Process of RPG-Loaded LNHS

The numerical analysis was accomplished via the Design-Expert software to optimize RPG-loaded LNHS by maximizing both responses in order to choose the optimal liponiosomal formula by simultaneous optimization of various response parameters via the desirability criterion. Higher desirability levels indicate closer proximity to the desired values.<sup>40,41</sup>

The optimal RPG-loaded liponiosomal formula was F7 because it had the greatest desirability (0.742). Therefore, additional characterization studies were conducted on it.

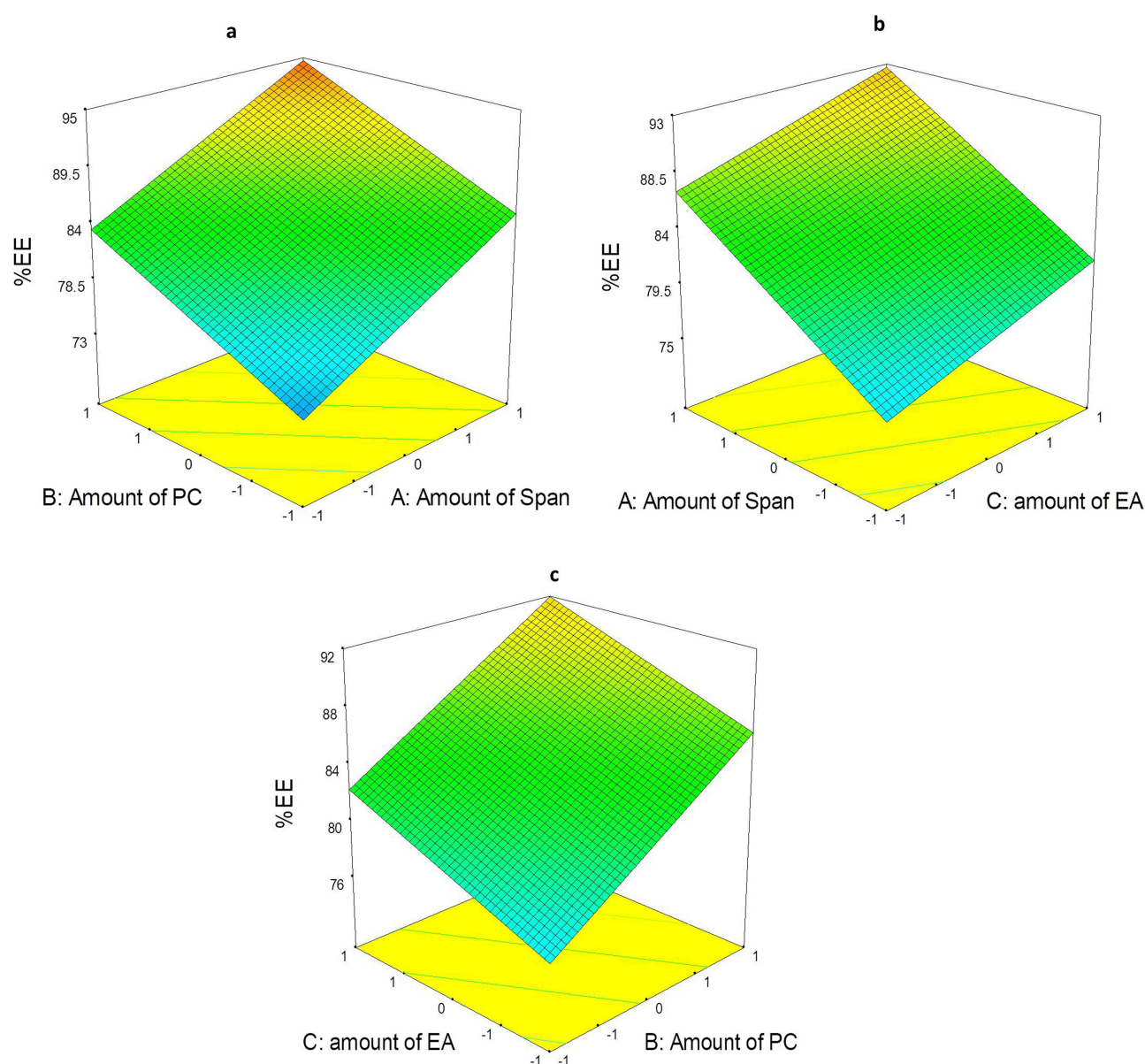


**Figure 10** 3D-response surface graph signifying the influence of different variables (a) X1, X2 (b) X1, X3 (c) X2, X3 on EE% of RPG-loaded LNHS. **Abbreviations:** RPG, Repaglinide; EE, encapsulation efficiency of RPG-loaded LNHS.

## Comparative Evaluation Between the LNHS and the Corresponding LVs and NVs

### Ex vivo Intestinal Permeability Study

The optimized RPG-loaded LNHS demonstrated significant progress in permeability ( $93.22 \pm 1.56\%$ ) than the free RPG dispersion ( $53.04 \pm 1.63$ ), the corresponding NVs ( $86.65 \pm 2.14\%$ ), and LVs ( $79.93 \pm 2.35\%$ ) (Figure 13). Moreover, the optimized RPG-loaded LNHS exhibited greater enhancement in the permeation parameters, Table 5. That might be explained by the synergism between the PC and Span within the lipid bilayer. These results align with those of Eaknai et al<sup>10</sup> who concluded that LNHS have improved the permeability of Fenugreek extract more than the free extract.

Besides, the presence of the EAs in the LNHS enhanced the elasticity, and henceforth, the permeation of the LNHS without rupture.<sup>13,42</sup>

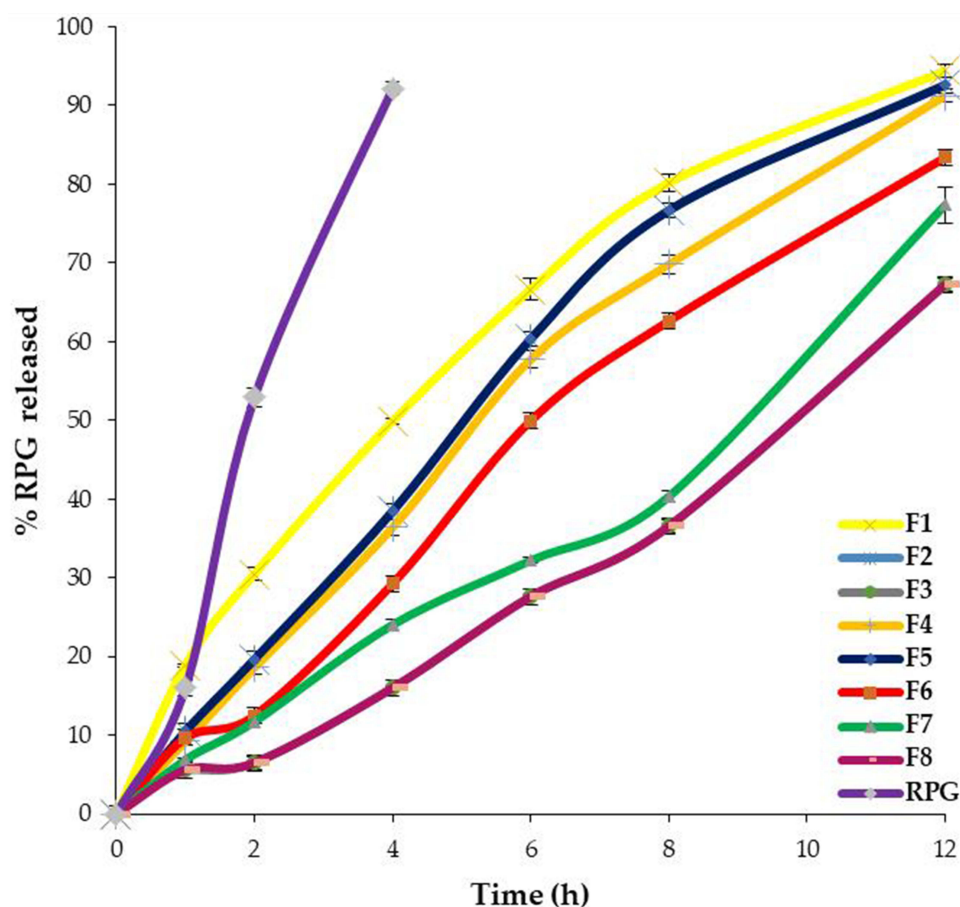
**Table 4** Validation of the Statistical Significance for the 2<sup>3</sup> Factorial Design of RPG-Loaded LNHS by ANOVA

Independent Variable	Source	Sum of Squares	Mean Squares	Degree of Freedom	F-Value	p-value
EE% (Y1)	Model	502.91	167.64	3	97.81	0.0003
	X1	251.22	251.22	1	146.57	0.0003
	X2	187.11	187.11	1	109.17	0.0005
	X3	64.58	64.58	1	37.68	0.0036
Q <sub>12h</sub> (Y2)	Model	279.94	93.31	3	45.32	0.0015
	X1	34.16	34.16	1	16.59	0.0152
	X2	172.89	172.89	1	83.96	0.0008
	X3	72.90	72.90	1	35.40	0.0040

**Notes:** Y1: Encapsulation efficiency %, Y2: Q<sub>12h</sub> of RPG-loaded LNHS, X1: Amount of Span, X2: Amount of PC, X3: Amount of EA.

## The Stability Test

Table 6 illustrates the % variation in different parameters between the fresh and the stored LNHS, LVs and NVs. For the LNHS, different parameters did not vary significantly ( $p > 0.05$ ). Conversely, the comparable NVs and LVs investigated

**Figure 11** %drug released from RPG-loaded LNHS and RPG dispersion across the cellulose membrane for 12 h.

**Abbreviations:** RPG, Repaglinide; LNHS, Liponiosomal hybrids of Repaglinide.

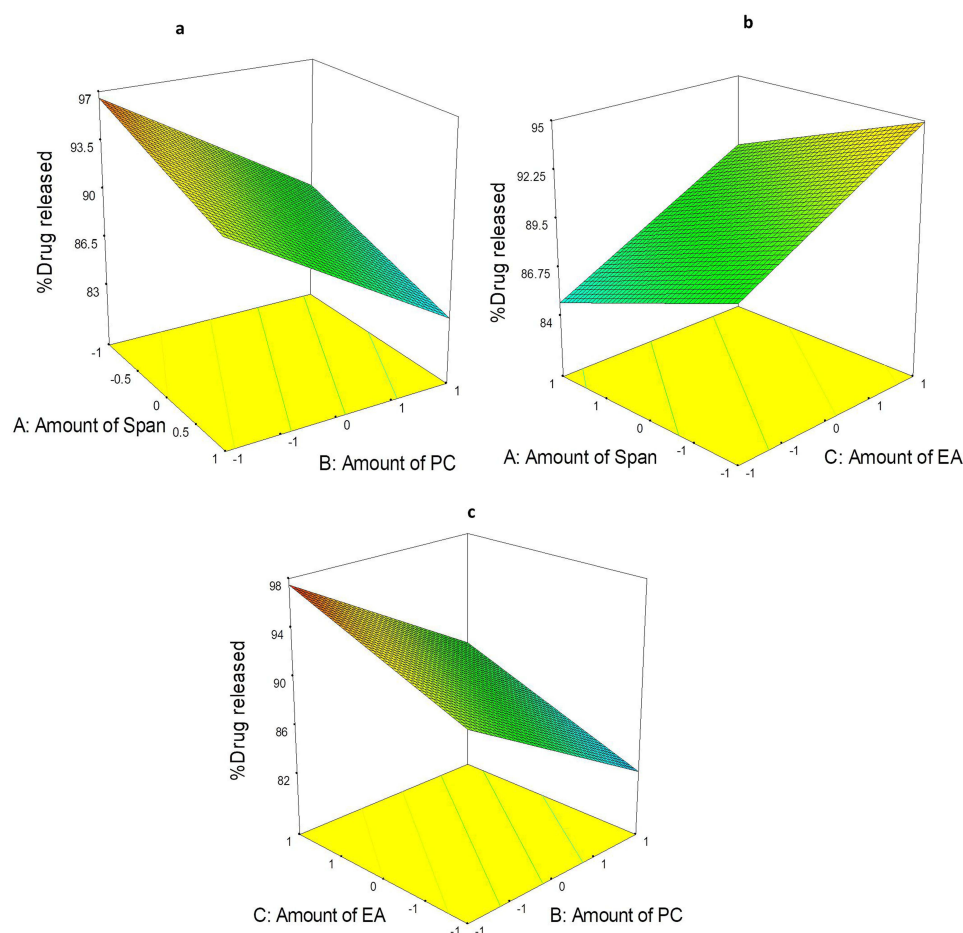


**Figure 12** 3D-response surface graph signifying the influence of different variables (a) X1, X2 (b) X1, X3 (c) X2, X3 on  $Q_{12h}$  of RPG-loaded LNHs. **Abbreviation:** RPG, Repaglinide; LNHs, Liponiosomal hybrids of Repaglinide.

a significant drop in the EE% ( $p < 0.05$ ), the drug content ( $p < 0.01$ ,  $p < 0.05$ ), and  $Q_{12h}$  ( $p < 0.01$ ,  $p < 0.05$ ), respectively. That could be attributed to the synergism between the liposomal and niosomal contents that improved both the vesicular integrity and the encapsulation of RPG.

## Characterization Tests of the Optimal LNHs of RPG

### Vesicle Size and Zeta Potential Estimation

According to data obtained from the dynamic laser scattering study, the average size of the optimal RPG-loaded liponiosomal formula was 334.9 nm, Figure 14 and their polydispersity index (PDI) was 0.356, demonstrating the low variation between the size of different RPG-loaded LNHs.<sup>19</sup> F7 has a zeta potential of  $-20.5$  mv, which shows that the liponiosomal nanovesicles are reasonably stable. This is because of the strong repulsive force and the high-energy barriers between them.<sup>7</sup>

### Studying the Morphological Properties by SEM

The SEM has verified the development of distinct and spherical RPG-loaded liponiosomal nanovesicles with smooth surfaces (Figure 15).

### Measurement of Elasticity of LNHs

The conventional LNHs lack deformability and may rupture during penetration via different membranes due to the absence of EAs.<sup>12</sup> The predicted DI of F7 ( $26.33 \pm 0.71$ ) was significantly greater than that of the corresponding LNHs



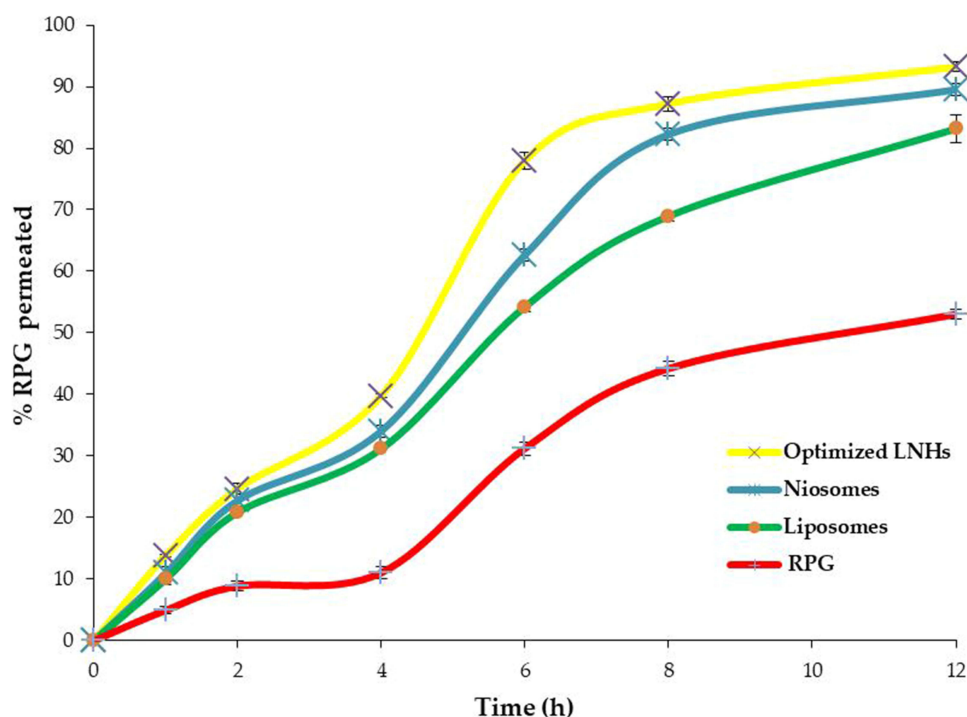


**Figure 13** The intestinal permeation of the optimal LNHs of RPG, free RPG, RPG-loaded liposomes and RPG-loaded niosomes.

**Abbreviations:** RPG, Repaglinide; LNHs, liponiosomal hybrids.

( $2.34 \pm 0.56$ ). The high DI value can efficiently describe the squeezing ability of RPG-loaded LNHs through the small gaps of different biological membranes with no rupture. The addition of EAs could improve the permeability of liponiosomal hybrids without disrupting the vesicular integrity.<sup>28,43</sup>

**Table 5** Comparing the Intestinal Permeation Parameters of the Optimal RPG-Loaded LNHs with the Corresponding LVs, NVs and the Free RPG

Formula	*Steady-State Flux ( $\mu\text{g}/\text{cm}^2 \text{ hr}$ )	*Permeability Coefficient (Cm/hr)	Enhancement Ratio
RPG dispersion	$3.60 \pm 0.13$	$0.0036 \pm 0.03$	—
LNHs	$11.24 \pm 1.46$	$0.0114 \pm 0.05$	3.12
LVs	$6.06 \pm 1.24$	$0.0061 \pm 0.12$	1.68
NVs	$7.66 \pm 0.48$	$0.0076 \pm 0.14$	1.47

**Note:** \*The values ( $n = 3$ ) designate the average  $\pm$  SD.

**Abbreviations:** RPG, Repaglinide; LNHs, liponiosomal hybrids; LVs, liposomes; NVs, niosomes.

**Table 6** Impact of 3 Months of Storage at  $4^\circ\text{C}$  on the Optimal RPG-Loaded LNHs NVs, and LVs

Parameter	% Change		NVs
	LNHs	LVs	
Drug content (%)	$1.93 \pm 0.03$	$16.98 \pm 0.02$	$12.71 \pm 0.03$
EE (%)	$2.18 \pm 0.03$	$12.56 \pm 0.09$	$10.11 \pm 0.07$
$Q_{12h}$ (%)	$1.17 \pm 0.04$	$15.96 \pm 0.05$	$11.45 \pm 0.04$

**Abbreviations:** RPG, Repaglinide; LNHs, liponiosomal hybrids; LVs, liposomes; NVs, niosomes; EE, encapsulation efficiency;  $Q_{12h}$ , % RPG released after 12 h.

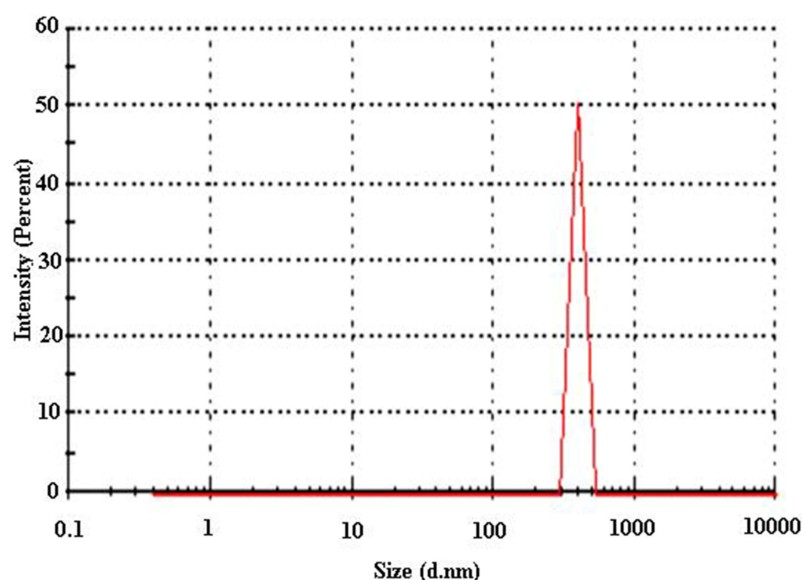


**Figure 14** The size distribution curve of the optimal LNHs of RPG (F7).

**Abbreviation:** RPG, Repaglinide; LNHs, Liponiosomal hybrids of Repaglinide.

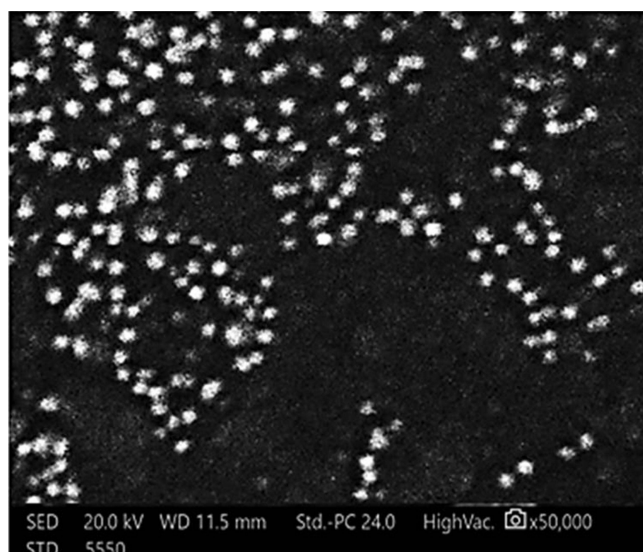


**Figure 15** Morphology of the optimized RPG-loaded LNHs by SEM.

**Abbreviations:** RPG, Repaglinide; LNHs, Liponiosomal hybrids of Repaglinide; SEM, scanning electron microscopy.

## Fourier Transform Infrared (FTIR) Spectroscopy of RPG-Loaded LNHs

The FTIR spectra of RPG, PC, CHO, Span 60, Tween 80, the physical mixture, and the optimized RPG-loaded LNHs are illustrated in Figure 16. RPG exhibited distinctive peaks at  $3305\text{ cm}^{-1}$  and  $1683\text{ cm}^{-1}$  corresponding to N-H and the carbonyl group stretching vibrations, respectively. The aromatic C = C bending and the N-H bending are both correlated to the bands at  $1630\text{ cm}^{-1}$  and  $1563\text{ cm}^{-1}$ , respectively.<sup>3</sup> The distinguishing peaks corresponding to CHO, indicative of –OH stretching, are found at  $3402\text{ cm}^{-1}$ . The detected peaks at  $2798\text{--}3000\text{ cm}^{-1}$  are ascribed to the CH<sub>2</sub> and CH<sub>3</sub> groups stretching vibrations.<sup>6</sup> With respect to PC, the spectrum showed representative peaks at  $1729\text{ cm}^{-1}$  (C=O stretching vibration), at  $1417\text{ cm}^{-1}$  (–CH<sub>3</sub> deformation), at  $1165\text{ cm}^{-1}$  and  $1033\text{ cm}^{-1}$  (PO<sub>2</sub> and P-O-C vibrations, respectively), and at  $700\text{ cm}^{-1}$  (C=C stretching vibration). For Span 60, prominent peaks appeared at  $3409\text{ cm}^{-1}$  (the aliphatic hydroxyl group),  $1741\text{ cm}^{-1}$  (the carbonyl stretch of ester), and  $2934\text{ cm}^{-1}$  (the C–H stretch).<sup>44</sup> The IR spectroscopy of Tween 80 demonstrated peaks at  $2905$  and  $2852\text{ cm}^{-1}$  related to the

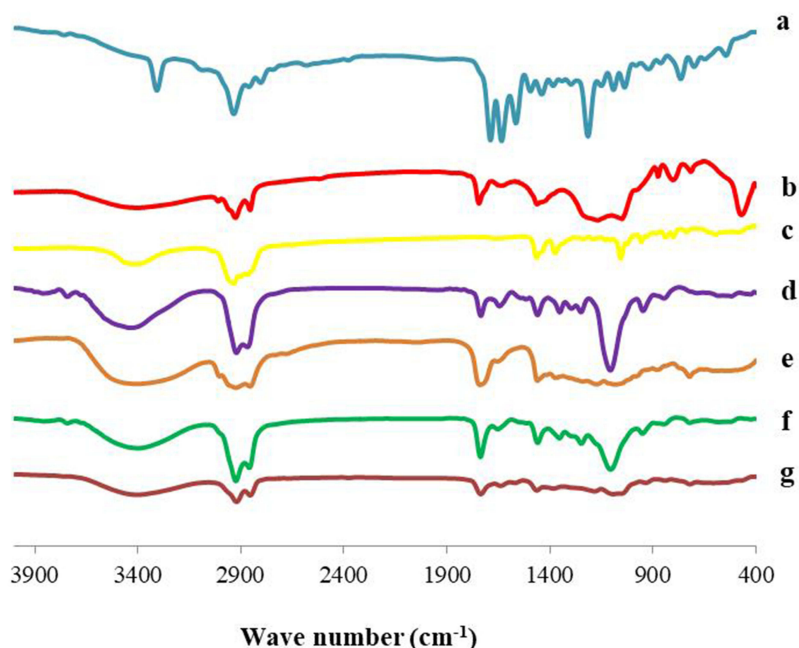


**Figure 16** FTIR spectra of (a) RPG, (b) PC, (c) CHO, (d) Tween 80, (e) Span 60, (f) physical mixture and (g) liponiosomal hybrid.  
**Abbreviations:** RPG, Repaglinide; PC, Phosphatidyl choline; CHO, Cholesterol.

stretching vibrations of methylene groups, the peak at  $1731\text{ cm}^{-1}$  could be attributable to the ester carbonyl group and the peak at  $3438\text{ cm}^{-1}$  is associated to the hydroxyl group.<sup>28,45</sup>

The index peaks of different excipients could be seen in the physical mixture's IR spectrum that explored the absence of any chemical bondings between RPG and the selected ingredients and they had only physical interactions. However, upon comparing the spectra of the physical mixture and RPG-loaded LNHs, it is worth mentioning that a shift and a decrease in the intensity of the distinctive peaks occurred within the RPG-loaded LNHs which could be attributable to the encapsulation of RPG within LNHs.<sup>5</sup>

## In vivo Study

As a type 2 DM model, STZ-induced experimental animals were employed. The pancreatic beta-cells that secrete insulin are selectively destroyed by STZ. RPG encourages pancreatic  $\beta$ -cells to release more insulin, which causes it to have an acute hypoglycemic effect.

Upon comparing the average serum glucose and the mean serum insulin with the diabetic control group, it is obvious that RPG (group III) produced a significant change ( $p < 0.05$ ) up to 2h post-doses, while RPG-loaded LNHs (group IV) investigated a more significant change ( $p < 0.01$ ) up to 12h post-dose with a higher maximum blood glucose lowering effect of  $61.63 \pm 4.6\%$  than free RPG ( $45.78 \pm 5.2\%$ ), **Figures 17 and 18**. The hypoglycemic response was still evident at the 12-h mark of the study, demonstrating a  $36.55 \pm 5.8\%$  reduction in blood glucose levels. In contrast, RPG treatment exhibited  $13.96 \pm 4.5$  blood glucose reduction. As a result, this leads to decreasing dose frequency and increasing patient compliance.

It can be inferred that the RPG-loaded LNHs have a higher hypoglycemic effect compared to free RPG, which could be explained on the basis of enhancing the intestinal absorption of RPG upon encapsulation within LNHs.<sup>7</sup> The above outcomes are in agreement with other researchers such as Eaknai et al<sup>10</sup> who investigated the role of LNHs in improving the efficacy of the tested drugs.

The oxidative stress is a significant factor in the development of cardiovascular complications associated with DM. Normal cellular respiration generates hydrogen peroxide which is responsible for pancreatic  $\beta$ -cell damage and insulin signaling inhibition. Various biochemical parameters can be employed to evaluate a compound's antioxidant activity. SOD is a primary antioxidant enzyme that transforms superoxide into hydrogen peroxide and molecular oxygen. Meanwhile, CAT primarily regulates hydrogen peroxide concentration, whereas GSH serves as another crucial antioxidant that helps prevent oxidative stress induced by reactive oxygen species.<sup>46</sup>

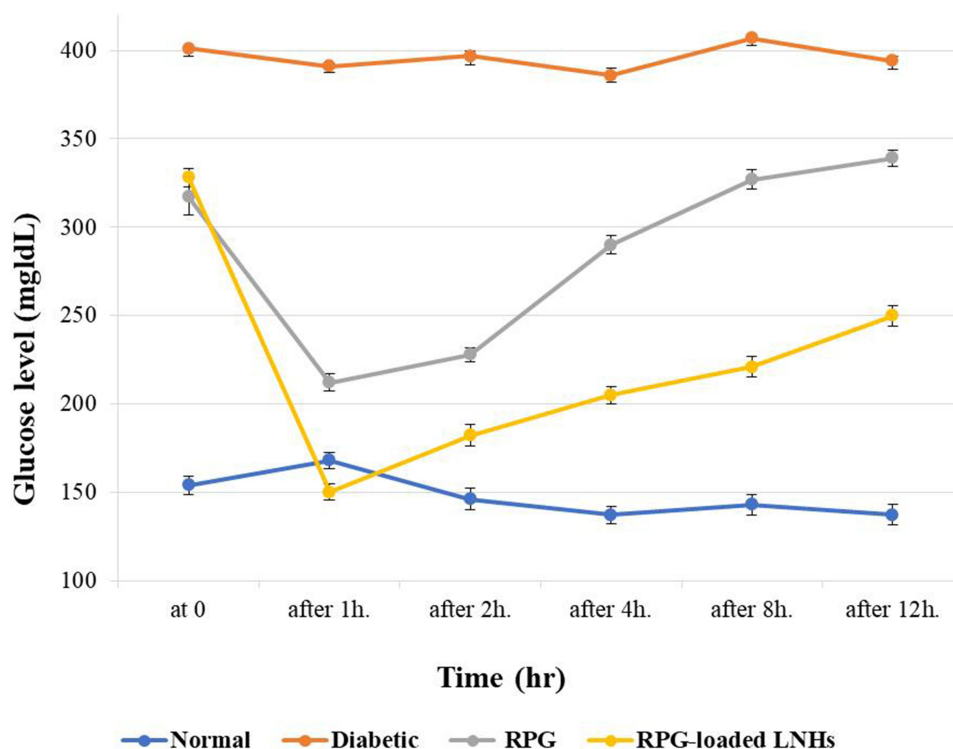


**Figure 17** The mean ( $\pm$ SD) serum glucose levels (mg/dl) of normal rats, diabetic control rats and those treated with pure RPG and RPG-loaded LNHs at different time intervals.

**Abbreviations:** RPG, Repaglinide; LNHs, Liponiosomal hybrids of Repaglinide.

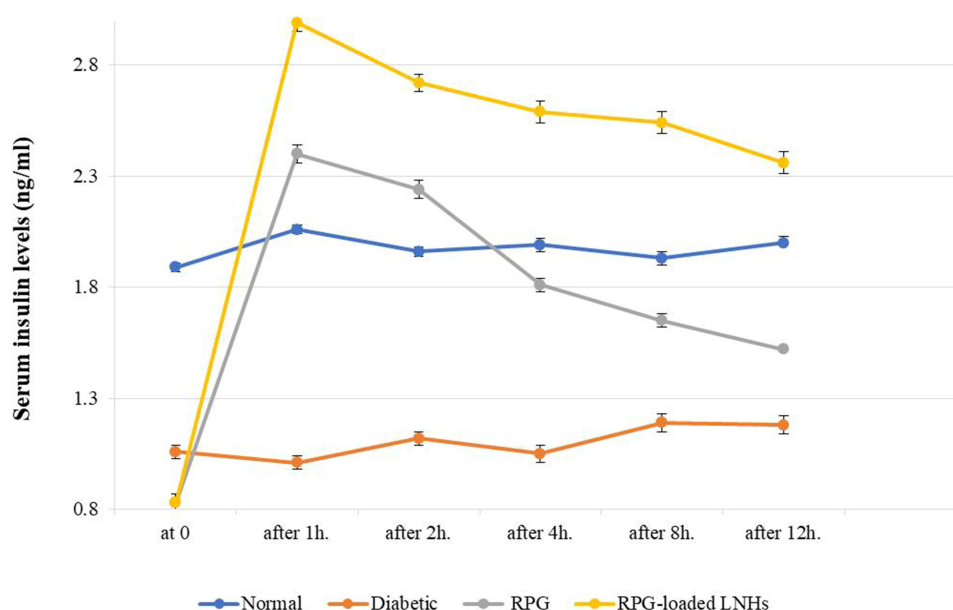


**Figure 18** The mean ( $\pm$ SD) serum insulin levels (ng/mL) of normal rats, diabetic control rats and those treated with pure RPG and RPG-LNHs at different time intervals.

**Abbreviation:** RPG, Repaglinide; LNHs, Liponiosomal hybrids of Repaglinide.

The change in the activity of the anti-oxidant enzymes in the pancreatic tissues of the rats in different groups is depicted in Figure 19. In STZ-induced diabetic rats, the LNHs-treated rats demonstrated a more significant ( $P < 0.01$ ,  $P < 0.001$ ) rise in SOD, CAT, and GSH than free RPG and control groups, respectively which demonstrated the higher antioxidant activity of the LNHs than free RPG, thereby supporting the utilization of RPG-loaded LNHs as an effective anti-oxidant in treatment of DM.

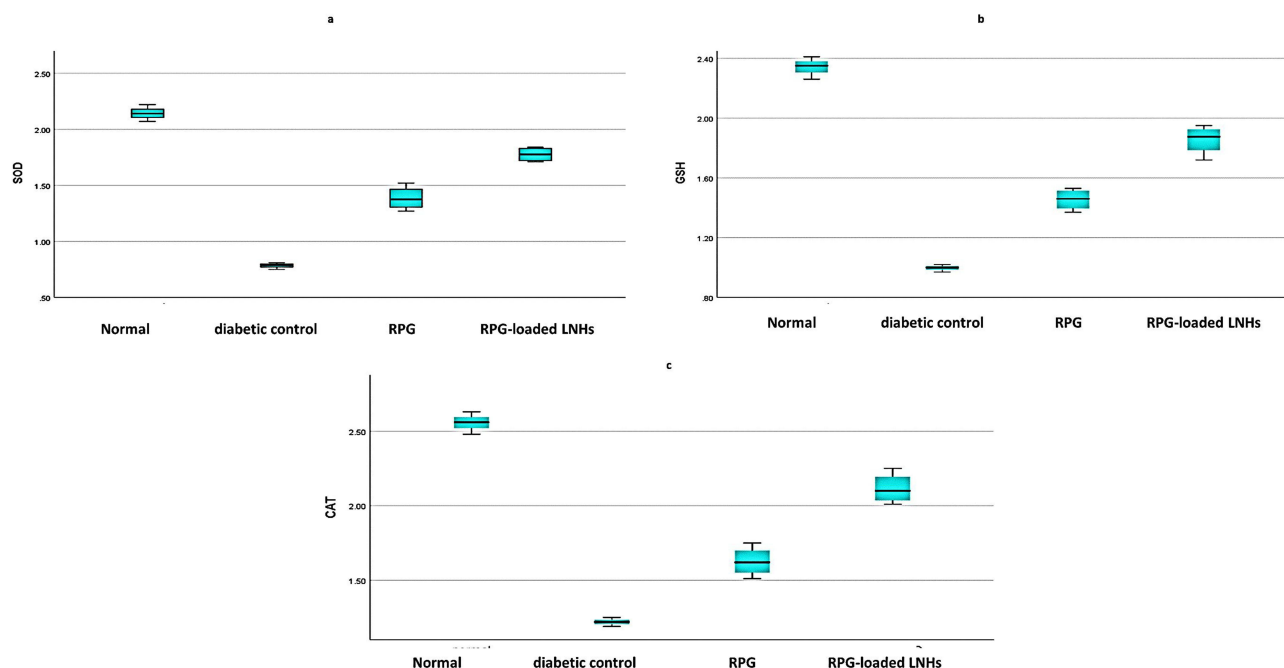


**Figure 19** The mean ( $\pm$ SD) levels of (a) SOD (U/mL), (b) GSH (mmol/L), and (c) CAT (U/L) in the serum of normal rats, diabetic control rats and those treated with pure RPG and RPG-loaded LNHS after 14 days of treatment.

**Abbreviation:** RPG, Repaglinide; LNHS, Liponiosomal hybrids of Repaglinide; SOD, Superoxide dismutase; GSH, glutathione; CAT, Catalase.

The pharmacokinetic investigation was carried out to assess the impact of encapsulating RPG into LNHS on its bioavailability. The absorption of RPG in rats was monitored by measuring the plasma concentrations over different time points, as depicted in Figure 20. A noticeable disparity in the plasma drug-profile can be observed, as indicated by the

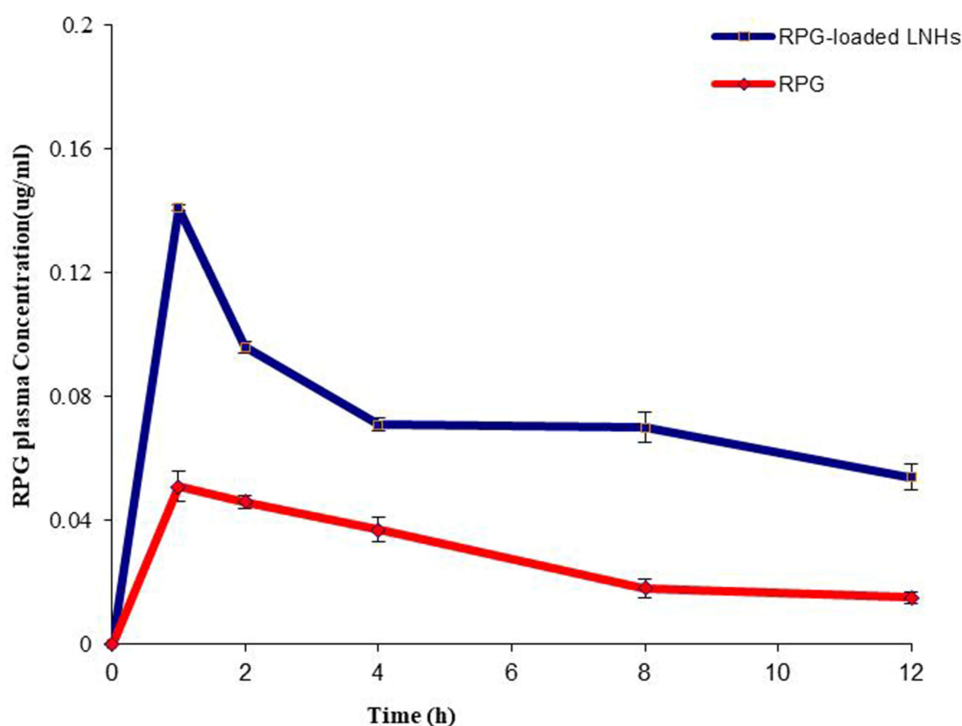


**Figure 20** The plasma concentration-time plot of RPG and RPG-loaded LNHS.

**Abbreviations:** RPG, Repaglinide; LNHS, liponiosomal hybrids.

rapid depletion of the plasma drug concentration for free RPG. However, the release of RPG from the RPG-LNHs persisted for 12 h. These results revealed the sustained release of RPG from LNHs, ultimately reducing administration frequency and enhancing patient compliance.

Moreover, the findings demonstrated that RPG-loaded LNHs exhibited a significantly ( $p < 0.001$ ) higher  $C_{\max}$  ( $0.14 \pm 0.022 \mu\text{g/mL}$ ) than the free RPG ( $C_{\max} = 0.05 \pm 0.014 \mu\text{g/mL}$ ). The elevated  $C_{\max}$  of RPG-loaded LNHs indicated an enhancement in RPG absorption through loading into the LNHs. The oral bioavailability improvement was also evident in the area under the curve ( $AUC_{0-24}$ ) results, which showed a significant ( $p < 0.01$ ) increase for the optimal RPG-loaded LNHs ( $AUC_{0-24} = 0.885 \pm 0.03 \mu\text{g.h/mL}$ ) compared to RPG ( $AUC_{0-24} = 0.332 \pm 0.02 \mu\text{g.h/mL}$ ).

The superior performance exhibited by the RPG-LNHs over RPG may be attributed to increased penetration capabilities of the LNHs due to the synergism between liposomal and niosomal contents.<sup>8</sup> Additionally, encapsulating RPG within LNHs boosted its stability by shielding it from enzymatic degradation.<sup>12</sup> These findings closely align with Pandey et al<sup>15</sup> who reported that the in vivo pharmacokinetic study revealed a 2-fold increase in bioavailability of RPG-loaded nanoparticles over RPG.

It is worthy noting that the deformable LNHs improved effectively both the hypoglycemic effect and bioavailability of RPG. Hence, LNHs are promising drug carriers for RPG.

## Conclusions

The present study has successfully illustrated the development of RPG-loaded LNHs, which serve as an innovative and adaptable nano-carrier capable of enhancing RPG's solubility, permeability, and bioavailability. Utilizing the reverse ethanol injection technique, the RPG-loaded LNHs were synthesized through a  $2^3$ -factorial experimental design, with the optimal LNHs (F7) being selected based on the highest desirability value. Moreover, when juxtaposed with unprocessed RPG, there was a noteworthy augmentation in the hypoglycemic effect. In conclusion, the integration of liposomes and niosomes within the LNH contributed to the establishment of a robust drug delivery platform adept at overcoming the challenges associated with RPG's inherently poor solubility and restricted bioavailability.

## Disclosure

The authors report no conflicts of interest in this work.

## References

- Madhav N, Yadav A. Development and evaluation of novel repaglinide biostrips for translabial delivery. *Int Res J Pharm*. 2013;4(5):198–202. doi:10.7897/2230-8407.04540
- Kumar G, Talsania M, Goli D, Karki R. Formulation and optimization of nanostructured lipid matrices of repaglinide using factorial design. *World J Pharm Pharm Sci*. 2013;2(6):5521–5537.
- Shravya Lakshmi S, Parthiban S, Senthil Kumar G, Tamizh Mani T. Development and evaluation of mucoadhesive liposomes of repaglinide for oral controlled delivery system. 2017.
- Yaghoobian M, Haeri A, Bolourchian N, et al. The impact of surfactant composition and surface charge of niosomes on the oral absorption of repaglinide as a BCS II model drug. *Int J Nanomed*. 2020;15:8767–8781. doi:10.2147/IJN.S261932
- Mohammadi M, Haghirosadat BF, Ehsani R, et al. Synthesis, characterization and evaluation of liponiosome containing ginger extract as a new strategy for potent antifungal formulation. *J Clus Sci*. 2020;31(5):971–981. doi:10.1007/s10876-019-01702-9
- Mazyed EA, Zakaria S. Enhancement of dissolution characteristics of clopidogrel bisulphate by proniosomes. *Int J Appl Pharm*. 2019;77–85. doi:10.22159/ijap.2019v11i2.30575
- Mazyed EA, Badria FA, ElNaggar MH, El-Masry SM, Helmy SA. Development of cyclodextrin-functionalized transethoniosomes of 6-gingerol: statistical optimization, in vitro characterization and assessment of cytotoxic and anti-inflammatory effects. *Pharmaceutics*. 2022;14(6):1170. doi:10.3390/pharmaceutics14061170
- Tripathi A, Rathore R, Chauhan C. Liponiosomal drug delivery system—a review. *J. pharm. sci. bio-sci. res*. 2013;3:100–104.
- Sasani E, Shahi Malmir H, Daneshmand F, et al. Synthesis and physiochemical characterizing of liponiosomal hybrid nano-carriers as carriers for doxorubicin hcl anti-cancer drug. *J Sabzevar Univ Med Sci*. 2020;27(1):35–47.
- Eaknai W, Bunwatcharaphansakun P, Phungbun C, et al. Ethanolic fenugreek extract: its molecular mechanisms against skin aging and the enhanced functions by nanoencapsulation. *Pharmaceutics*. 2022;15(2):254. doi:10.3390/ph15020254
- Badria FA, Abdelaziz AE, Hassan AH, Elgazar AA, Mazyed EA. Development of provesicular nanodelivery system of curcumin as a safe and effective antiviral agent: statistical optimization, in vitro characterization, and antiviral effectiveness. *Molecules*. 2020;25(23):5668. doi:10.3390/molecules25235668
- Mazyed EA, Helal DA, Elkhoudary MM, Abd Elhameed AG, Yasser M. Formulation and optimization of nanospanlastics for improving the bioavailability of green tea epigallocatechin gallate. *Pharmaceutics*. 2021;14(1):68. doi:10.3390/ph14010068



13. Gaafar PME, Abdallah OY, Farid RM, Abdelkader H. Preparation, characterization and evaluation of novel elastic nano-sized niosomes (ethoniosomes) for ocular delivery of prednisolone. *J Liposome Res.* 2014;24(3):204–215. doi:10.3109/08982104.2014.881850
14. Y-Q X, Chen W-R, Tsosie JK, et al. Niosome encapsulation of curcumin: characterization and cytotoxic effect on ovarian cancer cells. *J Nanomater.* 2016;2016:1–9.
15. Pandey SS, Patel MA, Desai DT, et al. Bioavailability enhancement of repaglinide from transdermally applied nanostructured lipid carrier gel: optimization, in vitro and in vivo studies. *J Drug Delivery Sci Technol.* 2020;57:101731. doi:10.1016/j.jddst.2020.101731
16. Sahu AK, Mishra J, Mishra AK. Introducing tween-curcumin niosomes: preparation, characterization and microenvironment study. *Soft Matter.* 2020;16(7):1779–1791. doi:10.1039/C9SM02416F
17. Farghaly DA, Aboelwafa AA, Hamza MY, Mohamed MI. Topical delivery of fenopufen calcium via elastic nano-vesicular spanlastics: optimization using experimental design and in vivo evaluation. *AAPS Pharm Sci Tech.* 2017;18(8):2898–2909. doi:10.1208/s12249-017-0771-8
18. Abd-Elal RM, Shamma RN, Rashed HM, Bendas ER. Trans-nasal zolmitriptan novasomes: in-vitro preparation, optimization and in-vivo evaluation of brain targeting efficiency. *Drug Deliv.* 2016;23(9):3374–3386. doi:10.1080/10717544.2016.1183721
19. Nasr M. In vitro and in vivo evaluation of proniosomes containing celecoxib for oral administration. *Am Assoc Pharma Sci.* 2010;11(1):85–89.
20. Bansal S, Aggarwal G, Chandel P, Harikumar S. Design and development of cefdinir niosomes for oral delivery. *J Pharm Bioall Sci.* 2013;5(4):318. doi:10.4103/0975-7406.120080
21. Mehanna MM, Motawaa AM, Samaha MW. Nanovesicular carrier-mediated transdermal delivery of tadalafil: i-formulation and physicochemical characterization. *Drug Dev Ind Pharm.* 2015;41(5):714–721. doi:10.3109/03639045.2014.900075
22. Hollands C. The animals (scientific procedures) act 1986. *Lancet.* 1986;2(8497):32. doi:10.1016/S0140-6736(86)92571-7
23. Kilkenny C, Browne WJ, Cuthill IC, Emerson M, Altman DG. Improving bioscience research reporting: the arrive guidelines for reporting animal research. *PLoS Biol.* 2010;8(6):e1000412. doi:10.1371/journal.pbio.1000412
24. Directive E. 63/eu of the European parliament and of the council of 22 September 2010 on the protection of animals used for scientific purposes. *Off J Eur Union.* 2010;276:33–79.
25. Sallam MA, Boscá MTM. Optimization, ex vivo permeation, and stability study of lipid nanocarrier loaded gelatin capsules for treatment of intermittent claudication. *Int J Nanomed.* 2015;10:4459. doi:10.2147/IJN.S83123
26. Jha SK, Karki R, Puttegowda VD, Harinarayana D. In vitro intestinal permeability studies and pharmacokinetic evaluation of famotidine microemulsion for oral delivery. *Int Schol Res Notice.* 2014;2014:1–7. doi:10.1155/2014/452051
27. Mady OY, Donia AA, Al-Shoubki AA, Qasim W, Zhou W. Paracellular pathway enhancement of metformin hydrochloride via molecular dispersion in span 60 microparticles. *Front Pharmacol.* 2019;10:10. doi:10.3389/fphar.2019.00010
28. Badria F, Mazyed E. Formulation of nanospanlastics as a promising approach for improving the topical delivery of a natural leukotriene inhibitor (3-acetyl-11-keto- $\beta$ -boswellic acid): statistical optimization, in vitro characterization, and ex vivo permeation study. *Drug Design Devel Ther.* 2020;14:3697. doi:10.2147/DDDT.S265167
29. Dooly M, Moore E, Cjr V. Research ethics. 2017.
30. Gheibi S, Kashfi K, Ghasemi AJB. A practical guide for induction of type-2 diabetes in rat: incorporating a high-fat diet and streptozotocin. *pharmacotherapy.* 2017;95:605–613. doi:10.1016/j.biopha.2017.08.098
31. Gadadare R, Mandpe L, V P. Ultra rapidly dissolving repaglinide nanosized crystals prepared via bottom-up and top-down approach: influence of food on pharmacokinetics behavior. *AAPS Pharm Sci Tech.* 2015;16(4):787–799. doi:10.1208/s12249-014-0267-8
32. Chao P-C, Li Y, Chang C-H, et al. Investigation of insulin resistance in the popularly used four rat models of type-2 diabetes. *Biomed Pharmacother.* 2018;101:155–161. doi:10.1016/j.biopha.2018.02.084
33. Yang DK, Kang HS. Anti-diabetic effect of cotreatment with quercetin and resveratrol in streptozotocin-induced diabetic rats. *Biomol Ther.* 2018;26(2):130. doi:10.4062/biomolther.2017.254
34. Cetto AA, Wiedenfeld H, Revilla MC, Sergio Iajjo E. Hypoglycemic effect of equisetum myriochaetum aerial parts on streptozotocin diabetic rats. *J Ethnopharmacol.* 2000;72(1–2).
35. Varshosaz J, Minayian M, Ahmadi M, E G. Enhancement of solubility and antidiabetic effects of repaglinide using spray drying technique in stz-induced diabetic rats. *Pharma Develo Technol.* 2017;22(6):754–763. doi:10.3109/10837450.2016.1143001
36. Van Herck H, Baumanns V, Brandt C, et al. Orbital sinus blood sampling in rats as performed by different animal technicians: the influence of technique and expertise. *Lab Ani.* 1998;32(4):377–386. doi:10.1258/002367798780599794
37. Jinno J-I, Kamada N, Miyake M, et al. Effect of particle size reduction on dissolution and oral absorption of a poorly water-soluble drug, cilostazol, in beagle dogs. *J Contro Rel.* 2006;111(1–2).
38. Zhang J, Froelich A, Michniak-Kohn B. Topical delivery of meloxicam using liposome and microemulsion formulation approaches. *Pharmaceutics.* 2020;12(3):282. doi:10.3390/pharmaceutics12030282
39. Mazyed EA, Abdelaziz AE. Fabrication of transgelosomes for enhancing the ocular delivery of Acetazolamide: statistical optimization, in vitro characterization, and in vivo study. *Pharmaceutics.* 2020;12(5):465. doi:10.3390/pharmaceutics12050465
40. Badria F, Fayed A, Ibraheem AK, et al. Formulation of sodium valproate nanospanlastics as a promising approach for drug repurposing in the treatment of androgenic alopecia. *Pharmaceutics.* 2020;12(9):866. doi:10.3390/pharmaceutics12090866
41. John B. Application of desirability function for optimizing the performance characteristics of carbonitrided bushes. *Int J Ind Eng Comput.* 2013;4(3):305–314. doi:10.5267/j.ijiec.2013.04.003
42. Salama HA, Mahmoud AA, Kamel AO, Abdel Hady M, Awad GA. Brain delivery of olanzapine by intranasal administration of transfersomal vesicles. *J Liposome Res.* 2012;22(4):336–345. doi:10.3109/08982104.2012.700460
43. Leonyza A, Surini S. Optimization of sodium deoxycholate-based transfersomes for percutaneous delivery of peptides and proteins. *Int J Appl Pharm.* 2019;329–332. doi:10.22159/ijap.2019v11i5.33615
44. El-Sayed MM, Hussein AK, Sarhan HA, Mansour HF. Flurbiprofen-loaded niosomes-in-gel system improves the ocular bioavailability of flurbiprofen in the aqueous humor. *Drug Dev Ind Pharm.* 2017;43(6):902–910. doi:10.1080/03639045.2016.1272120
45. Ren W, Tian G, Jian S, et al. Tween coated nayf 4: yb, er/nayf4 core/shell upconversion nanoparticles for bioimaging and drug delivery. *Rsc Adv.* 2012;2(18):7037–7041. doi:10.1039/c2ra20855e
46. Alam MS, Ahad A, Abidin L, et al. Embelin-loaded oral niosomes ameliorate streptozotocin-induced diabetes in Wistar rats. *Biomed Pharmacother.* 2018;97:1514–1520. doi:10.1016/j.biopha.2017.11.073

## International Journal of Nanomedicine

Dovepress

**Publish your work in this journal**

The International Journal of Nanomedicine is an international, peer-reviewed journal focusing on the application of nanotechnology in diagnostics, therapeutics, and drug delivery systems throughout the biomedical field. This journal is indexed on PubMed Central, MedLine, CAS, SciSearch®, Current Contents®/Clinical Medicine, Journal Citation Reports/Science Edition, EMBase, Scopus and the Elsevier Bibliographic databases. The manuscript management system is completely online and includes a very quick and fair peer-review system, which is all easy to use. Visit <http://www.dovepress.com/testimonials.php> to read real quotes from published authors.

Submit your manuscript here: <https://www.dovepress.com/international-journal-of-nanomedicine-journal>